

I appreciate the value that the reviewers and AE have found in the revised version of the paper, which demonstrates the likely role of topographically induced stress on potential soil production rates in the SGM. I thank everyone for all their hard work, which I think has made for a much improved paper.

Q: *“Please explain what the “average slope” as defined by Heimsath means, i.e. how it is calculated and whether this is an appropriate measure to relate to local stress intensity (all three reviewers comment on that point)”*

A: *Regarding the first issue, i.e., whether the average slope in the model is equivalent to the average slope as calculated by Heimsath et al.:*

It is clear from the context of their work that the average slope calculated by Heimsath et al. is an average of the gradients of hillslopes surrounding each sample location over a spatial scale that includes ridgetops and side slopes. I don't know precisely what spatial scale Heimsath et al. used for averaging, but it appears to be ~1 km. This is corroborated by patterns in the data, e.g., there are several clusters of samples (e.g., SG-105 to 108, SG-110 to 113) with individual data points separated by less than approximately 1 km that have precisely the same average slope value.

I emailed Arjun to ask for additional information on how he computed average slope. He noted that his calculation used only hillslope patches (valley bottoms were excluded) and graciously agreed to check his notes and get back to me with more details. By the time of the revision deadline (including an extension to the deadline), I had not heard back from him. When I receive his reply I will add the information he sends if there is still time.

In any case, I believe the average slope I use in the modeling is equivalent to the average slope computed by Heimsath et al. (2012). As stated in the manuscript, the average slope in the model is computed from the ridgetop to the steepest point in the model geometry. In the SGM, as in any region of narrow, V-shaped valleys, the steepest portion of the hillslope tends to occur at or near the base of the slope. Heimsath et al. computed average slopes from the ridgetops to the base of slopes (valley bottoms were excluded) over a spatial scale that included ridgetops and sideslopes. As such, the calculations are consistent.

I have added the following text on this issue:

*“The average slope computed from the model geometry is consistent with the average slope computed by Heimsath et al. (2012). The average slope in the model is computed from the ridgetop to the point of maximum slope in the model geometry. In the SGM, as in any region of narrow, V-shaped valleys, the steepest portion of the hillslope tends to occur at or near the base of the slope. Heimsath et al. (2012) computed their average slope from hillslope patches (valley bottoms were excluded) over a length scale that included ridgetops and side slopes. As such, the calculations are consistent.”*

*Regarding the second issue, i.e., whether average slope is the appropriate variable for quantifying local stress intensity:*

I tried hard in the previous version of the paper to emphasize that local stress intensity is a function of both slope and curvature. However, the reviewers are correct that more clarity was needed on this issue. I have included the following text in the revision:

*“It is important to note that the local stress modification in the Savage and Swolfs (1986) model is a function of both the local curvature and the slope averaged over a spatial scale that*

includes ridgetops and side slopes. Within an individual hillslope, local curvature controls the sign of stress modification, with extension occurring beneath ridgetops and compression beneath valley bottoms. The extension that occurs beneath ridgetops is the most important response of the model for the purposes of this paper since all of the Pr data come from locations at or near ridgetops (i.e., 24 of the 58 data points are on ridgetops, with the remaining data points located within approximately 100 m from ridgetops). The magnitude of the extension near ridgetops is controlled by the landscape-scale slope (quantified by Savage and Swolfs (1986) as  $b/a$ ), the slope averaged over a length scale that includes ridgetops and side slopes is the variable most consistent with  $b/a$ .” And to the discussion section I have added:

“Savage and Swolfs (1986) used a convex-concave geometry, defined by a conformal transformation, in which the slope increases linearly with distance from the divide to the steepest point on the hillslope. In higher-relief portions of the SGM characterized by more planar hillslopes, slopes increase abruptly over a relatively short distance from the ridgetop, then more slowly with increasing distance from the ridgetop. This difference introduces some uncertainty into the application. The model might overestimate the magnitude of topographically induced stress in high-relief portions of the SGM because a more planar slope has a lower curvature than a more parabolic slope and larger curvatures tends to increase extensional stress. On the other hand, more planar hillslopes localize curvature near the ridgetops, which might tend to increase bending stresses that drive extension over and above that predicted by the model for locations near ridgetops.”

*Q: “Please respond or take into account the second point made by Reviewer 1 who disputes your argument that the relationship between slope and production rate is due to extensional stress fracturing”*

A: Please note that I did not argue that the relationship between slope and production rate is due to extensional stress fracturing. Rather, I stated that the rocks in the SGM are pervasively fractured and that extension can open up those pre-existing fractures. See my responses to reviewer 1 for detailed responses to his/her concerns.

*Q: “Could you easily check whether hill orientation with respect to the regional steps field direction plays (or not) a role in setting production rate (through stress fracturing) as suggested by Reviewer 2; this is a good test of your hypothesis and, in my opinion, would not require much work to verify”*

A: I did not find a relationship between Pr values and local slope aspect (except for the tendency for lower Pr values to occur on north-facing slopes compared to south-facing slopes, which remains unexplained but could be related to the fact that south-facing slopes are steeper, on average, compared to north-facing slopes (see figure below)) or the orientation of the closest ridgeline.

This might appear to be evidence against the hypothesis of the paper. However, bear in mind that a topographic profile along the principal stress direction that runs through any sample location (even a sample location with a local ridgeline nearly parallel to the principal stress direction) will exhibit substantial topographic variability (increasing with average slope) since ridgelines do not run in straight lines. That is all that is required for compressive stress reduction

near ridgetops, i.e., that the sample location be in a relatively high topographic position in a region of moderate to high relief along the direction of principal stress. Topography is (to some extent) fractal, such that the local ridge-and-valley profile is embedded within larger-scale topographic variations, all of which contribute to the topographically induced stress (although local scales are more important because average slope and curvature values, which control the magnitude of compressive stress reduction, decrease with increasing spatial scale). Further complicating any simple test of how  $Pr$  values might correlate with the orientation of the nearest ridgeline with respect to the principal stress direction is the fact that simply identifying which is the local ridgeline can be unclear, as sample locations often sit in saddles between two ridgelines that run in perpendicular directions (see example below).

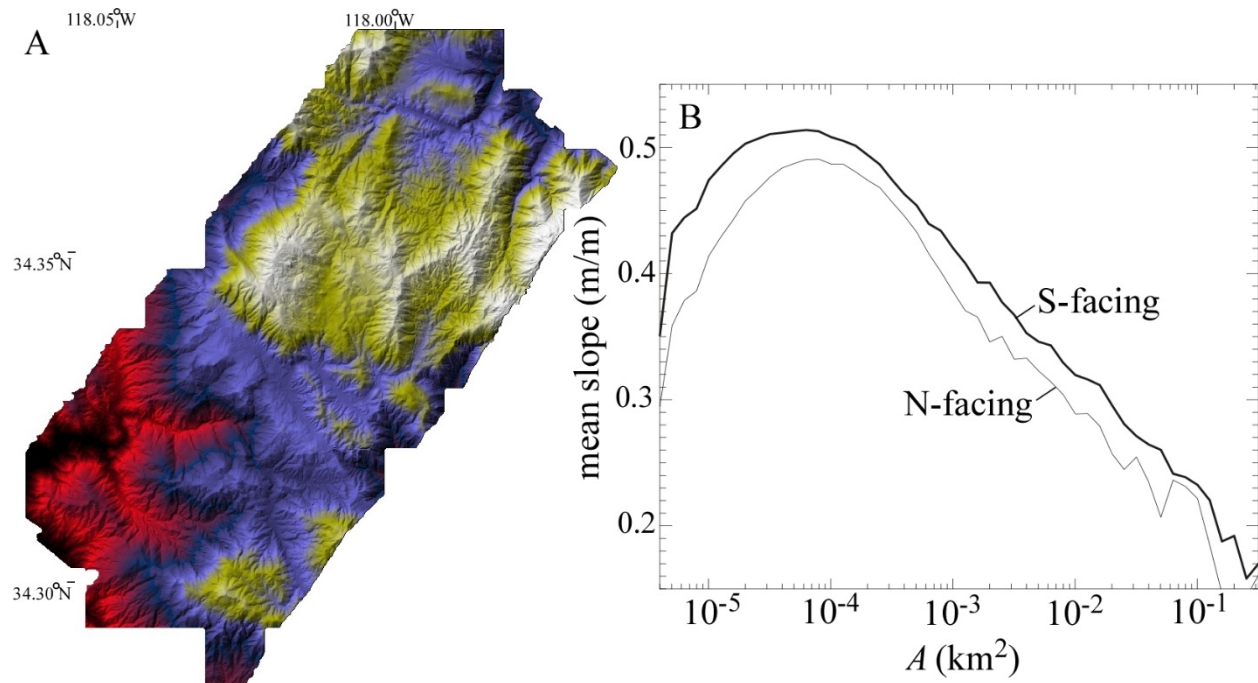


Figure. Demonstration that south-facing slopes are, on average, steeper than north-facing slopes in the SGM. (A) Shaded relief image of the only publically available lidar for the SGM. (B) Plots of the slope-area relationship derived from the DEM in (A), with south- and north-facing slopes considered separately.

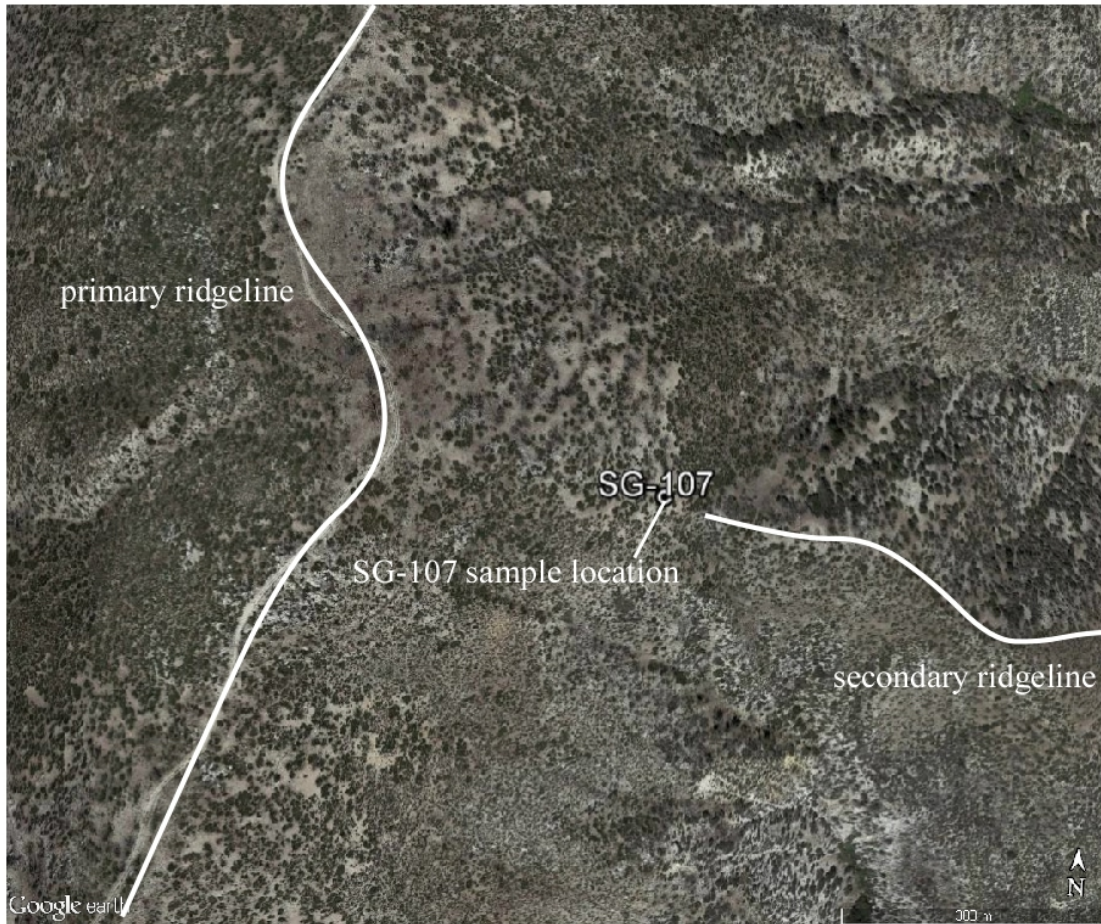


Figure. Demonstration of some of the complexity involved in trying to test how the orientation of the hillslope and/or nearest ridgeline with respect to the principal stress direction might control Pr values. In this case, the sample location exists within a saddle between a prominent ridgeline that runs SW-NE and a smaller (but closer) ridgeline that runs W-E.

Q: *“Please pay attention to the various remarks concerning the applicability of the Savage and Swolfs relationship to the study area, as well as the use of a correct measure of slope (see my first point. Reviewer 3 makes very constructive points concerning the way you have analyzed the data; the Reviewer’s suggestions should help clarify your approach and help supporting your interpretation. Reviewer 3 also makes a very interesting suggestion concerning the important section 2.2 of your manuscript; I urge you to consider this point carefully and, if possible, implement his suggestion(s) in your revised manuscript.”*

A: See responses below. Note that in some cases I did not agree with the suggestions of reviewer 3, but in all such cases I have provided very specific reasons for not doing so, which I hope the AE finds compelling.

**Reviewer 1 (denoted reviewer 3 in system):**

Q: “P2 line 2: “relatively uncommon in granitic rock types.” This needs a citation.”

A: Rephrased: “Slope failures in bedrock or intact regolith are common in some fine-grained sedimentary rocks (e.g., Griffiths et al., 2004; Roering et al., 2005) but may be less common in massive lithologies such as granite.”

Q: “P3, line 4-5: This is strange wording.  $P_r$  is the limit to soil production, and earlier it is stated that this limits erosion. Here  $P$  and  $E$  are said to greatly exceed  $P_r$ . I’m sure this statement is being used to highlight that  $P_r$  is in fact not the limit to soil production but I feel there should be a phrase or some rewording that makes this intention (if that is the intention) clear. A simple insertion of “apparent  $P_r$ ” might do the trick.”

A: The sentence does not state that  $P$  and  $E$  greatly exceed  $P_r$  values. The sentence states that  $P$  and  $E$  values from rapidly eroding portions of the range exceed  $P_r$  values from slowly eroding portions of the range, which is correct as stated.  $P_r$  values from one area do not necessarily limit soil production in other areas, because  $P_r$  values can and almost certainly do vary spatially.

Q: “P5, line 10-12: Not all ridges in the field site are oriented perpendicular to the most compressive stress direction. There are even a few oriented parallel. How does this affect the model prediction? I’m curious if one might expect a different signal depending on the orientation of the ridgelines. Note: I doubt one could see something like that in the data given the noise, but I think it is worth commenting upon.”

A: See response to AE’s request for a similar test.

Q: “P5, lines 13-15: The Savage and Swolfs paper is quite dense but they impose a particular geometry to their ridges. It isn’t clear to me if the ridges they model have geometry similar to the ridges in the field area, and thus it isn’t clear if the relationship between their maximum slope and average slope can be meaningfully applied to the field site. Their ridges look somewhat Gaussian (they are not, but they are convexo-concave), whereas in the San Gabriels the hillslopes have a short wavelength convexity at the top and are linear on the side slopes. Some comment should be made about how the Savage and Swolfs model is an approximation of real topography and how uncertain the stress field of real landscapes is as a result of differences between real landscapes and their idealised landscape. P5, line 15: While I do think converting an average slope into a specific slope in the Savage and Swolfs model is something of an approximation, I do find this connection between the switch from compression to tension fascinating.”

A: I agree with the reviewer that hillslopes in the high-relief portion of the SGM have a short wavelength convexity at the top and are more linear on the side slopes than the model geometry of S&S. However, lower-relief portions of the SGM (which are also represented in the dataset) have hillslopes that are more nearly parabolic, and hence more similar to the Savage and Swolfs geometry. I have addressed this concern with the following text: “Savage and Swolfs (1986) used a convex-concave geometry, defined by a conformal transformation, in which the slope increases linearly with distance from the divide to the point of maximum slope. For the specific mathematical model of Savage and Swolfs (1986), the average slope computed from the ridgetop to the point of maximum slope is equal to  $b/4a$ . In higher-relief portions of the SGM characterized by more planar hillslopes, slopes increase abruptly over a relatively short distance from the divide, then more

slowly with increasing distance. This difference introduces some uncertainty into the application. The model might overestimate the magnitude of topographically induced stress in high-relief portions of the SGM because a more planar slope has a lower curvature than a more parabolic slope, and larger curvatures tends to increase the magnitude of compressive stress reduction. On the other hand, more planar hillslopes localize curvature near the ridgetops, which might tend to increase the bending stresses that drive compressive stress reduction near ridgetops (where all of the sample locations come from) over and above that predicted by the model.”

Q: “P6, line 3: *Something I do not understand is that in the Savage and Swolfs paper, the horizontal and shear stresses vary substantially as a function of position (e.g., their figure 4). There is not much variation in  $\sigma_{xx}$  in figure 3 here. If these stresses vary horizontally (from ridgetop to channel) then if these stresses are affecting soil production rates they should do so to different extents on different parts of the hillslope, should they not? I suggest some clarification here.*”

A: Agreed. In the revised paper I have modified the text in several places to clarify that compressive stress reduction is maximized under ridgetops.

Figure 3 of Savage and Swolfs varies more substantially because their figure includes the entire shape of the ridge-valley transect, while I include only the ridge portion (because all of the Pr data are from near-ridge locations and because valleys in the SGM are V-shaped, not U-shaped as Savage and Swolfs assume).

Q: “P6, line 17: *Does this model do better than a simple linear fit? Again, I think this is an interesting approach but the model described by equation (4) has 4 parameters that must be fit to the data (and this excludes modifications for climatic influences).*”

A: I have demonstrated in the revision that the equation is more accurate than a linear fit, even accounting for the larger number of parameters (using a reduced chi-squared measure). Sentence added: “The null hypothesis that Pr,S values can be fit as well or better by a linear relationship can be rejected: the reduced- $\chi^2$  value, which takes into account different numbers of degrees of freedom, of the log-transformed values of equation (5), is less than half (45%) of the reduced- $\chi^2$  for a least-squares linear fit.”

Q: “Page 12 lines 6-7: *Clunky sentence. I suggest rewriting.*”

A: Reworded: “Stepwise regression is the process of computing the residuals of a regression and testing for additional controls, via additional regression and the calculation of a new set of residuals, until no additional explanatory variable can be identified. Stepwise regression is one method for testing the residuals of a regression for additional controls, which is a recommended step in all regression analyses.”

Q: “Page 13 line 9-11: *The thresholding behaviour is particularly interesting in light of the results presented earlier in the paper and it would be useful to specifically mention the previous authors in addition to Savage and Swolfs that found this behaviour.*”

A: I don’t know of any other studies that specifically found a threshold relationship between slope and some measure of topographically induced stress other than Savage and Swolfs.

Q: “Page 13, lines 16-17: I’m not sure if this sentence is a reflection of the content of the paper. The paper does not show stresses cause fractures which then lead to enhanced weathering. What it shows is that previous models of topographically-induced stresses suggest transitions from compressive to tensile strength at hillslope angles similar to those at which  $P_r$  values increase. This study doesn’t present fracturing data. I think this section needs more cautious language because at the moment it is describing processes that aren’t really addressed in the paper.”

A: The manuscript merely stated that the results suggest that stresses cause fractures which then lead to enhanced weathering. I think this is correct as written. However, I have adopted the reviewer’s suggestion and modified this sentence to: “The results presented here show that previous models of topographically induced stresses suggest transitions from compressive to tensile strength at hillslope angles similar to those at which  $P_r$  values increase. This similarity suggests that in the SGM, the release of compressive stress in steep landscapes may cause fractures beneath ridges to open, thereby allowing weathering agents to penetrate into the bedrock or intact regolith more readily.”

**Reviewer 2 (4 in system):**

Q: “It is not clear to me that the extensional stresses that are being invoked are occurring where the soil production rates are being measured. The average slope is used in both this study and in Heimsath et al., 2012. Average slope is measured as the average from the ridgetop to the maximum slope here, but I am not sure that this is how Heimsath et al., measured it (“the average slope over hillslopes adjacent to each sample location” is not clear. More importantly, the Savage and Swolfs model suggests that the maximum extension should be occurring on the ridgetop above the steep slopes, not on the steep slopes themselves (e.g. page 13 line 16). It seems that some of Heimsath et al.’s data were indeed collected from ridgetops, but some samples came from the steep hillslopes below them. The implication of the S&S model is that the maximum extension (and hence maximum  $S_r$  in this approach) should occur on ridgetops and not on steep hillslopes. Since ridgetops are, by definition, less steep than the surrounding hillslopes, this would negate the assertion that soil production rates are fastest on steep slopes because of extensional stress. It is possible that this is just a question of definitions, but if so then it needs to be explained further.”

A: Please see response to AE’s comment #1.

Q: “The correspondence of EVH to  $P_r/P_r,S$  is not convincing. The similarity is only marginal and is controlled by four points at high elevation. Related to this, I am not sure that it is appropriate to say that temperature limitations can be determined. The climatic index (equation 5) is somewhat arbitrary and could be expanded upon.”

A: Without more information from the reviewer it is difficult to know how my analysis could be improved to make it more convincing to him/her. I think it is highly significant that vegetation height shows a similar “hump” to that of  $P_r/P_r,S$ , although I acknowledge that the humps are offset by approximately 300 m. Some differences between the curves are to be expected due to the fact that EVH is influenced by the recent fire history, which temporarily reduces EHV in locations that have experienced fire in recent decades. Still, over a 1-km range of elevations, both EHV and  $P_r/P_r,S$  exhibit broadly similar increases and then decreases that suggest a causal connection

between vegetation cover and weathering rates. The alternative hypothesis (i.e., that Pr values are unrelated to vegetation cover) does not seem more plausible to me.

The results of the cluster analysis demonstrating climatic control at high elevations of the SGM are statistically significant even though they are based on just four data points (i.e., they are significant because all four points are so much lower than the Pr/Pr,S at lower elevations). The reviewer claims that this result is marginal. Is he/she suggesting that I adopt a significance level higher than the standard threshold of 95% or does he/she just not believe the result?

Regarding the reviewer's statement that my manuscript concluded that temperature limitations on Pr can be determined, please note that the manuscript stated only that the results were likely (not definitively) the result of temperature limitations (except for a somewhat firmer statement in the abstract that has been reworded). See also my response to reviewer 3 on this point.

Q: *“One of the other main issues is the assertion of a causal link between fracture opening and soil production (end of section 2.1). I do not accept that the results show a causal relationship between hillslope gradient and soil production rate through extensional stress fracturing (or reactivation). The higher R2 for Pr to Pr,pred than Pr to D only shows that the topographic stress fracture model provides a better correlation than fault damage model, but it could be that a third, unaccounted for, variable is the causal link. It is, however, an interesting thought experiment that is shown to be consistent with existing soil production data. If presented in such a format, Pelletier could present predictions, providing a powerful tool for guiding future soil production rate studies. This would involve restructuring the paper around the concept of topographic stress fracturing and the implications for the real world. Much of this is already included. It would be particularly useful for the community a set of testable model predictions were presented.”*

A: This concern is echoed by reviewer 3 (Simon Mudd), who suggested a rewording of Page 13, lines 16-17 to soften/clarify the conclusions. In addition to rewording on p. 13, I have carefully checked the manuscript to make sure that I have not claimed a definitive causal relationship between hillslope gradient and Pr values via topographical stress fracture opening (rather, the results are merely consistent with this hypothesis). The reviewer is correct that there could be some third control, related to slope but unrelated to topographically induced stress. However, in geosciences we always face the problem that a correlation between two variables that we explain by some mechanism (one that, in this case, has a solid foundation in theory) could, instead, be due to some other mechanism. Absent any suggestion of an alternative mechanism from this or any other reviewer, I think I have done the best I can (i.e., I cannot disprove all possible alternative hypotheses, particularly if none are identified).

Q: *“I am confused by the sentence on lines 3-4 of page 11. If the SGM is characterised by an exponential soil production function, then the maximum soil production rate (and presumably at least some erosion) should occur when there is no soil cover. If that is the case, then there is no need to presume that soil ever existed at the h=0 sites.”*

A: The distinction I am making is between persistent soil cover (soil that can be measured on any given day by a visit to the site) and episodic soil cover (soil that forms and persists only as long as it takes for it to be transported down the slope, which may be only seconds). As stated in the manuscript, soil (i.e., mobile debris) must be present in order for erosion to occur. This is clear

from the fact that immobile regolith, by definition, does not erode physically (i.e., it is immobile). In order for the landscape to erode, some mobile debris must be present, though it may only be present for seconds until rockfall or some other type of mass wasting moves it down the slope. I have tried to clarify this point by rewording the sentence to: “Here I use a soil-depth-independent transport relation because such models are highly sensitive to the presence/absence of soil and areas of thin or no soil are likely to have episodic cover (e.g., rapid mass wasting following incipient soil production) that makes measuring or estimating long-term averaged soil depths difficult.”

Q: “Terminology is not consistent throughout. Both Pr and P0 are used.”

A: Fixed.

Q: “Pg 14 line 5 – Should say “If soil production rates...”.”

A: Typo corrected.

**Reviewer 3 (5 in the system):**

Q: “In the entire manuscript, both soil and regolith seems to be interchanged. It would be good to choose one of them and explain why because they are not the same.”

A: I am confused by this comment, which notes that the two terms are not the same yet asks me to choose just one. Weathered material above fresh bedrock is comprised of *intact regolith* and *soil*. Both terms must be used in the context of describing the process of fresh bedrock breakdown into soil because intact regolith is the intermediate state between the two. Please note that the word regolith never appears in the manuscript without the modifier “intact” in front of it.

Q: “p2: line 10: I would rather say: between 100 and 2500m/Myr.”

A: Removed.

Q: “Pelletier proposed an alternative approach to analyze soil production rates obtained from CRN data. Rather than regressing the soil production function through all the data, the residual Pr is calculated separately for all the measured P values using h0 values as obtained from the regressions in the Heimsath et al. paper in 2012. I see no harm in this approach to test for additional controls on SPR. However, even in this revised manuscript, at some points I still feel uncomfortable with the way these Pr data are further analyzed.”

A: Calculating residuals *requires* first regressing the soil production function through all the data (as a first step). Therefore, I disagree with the reviewer my analysis is an alternative to regressing the soil production function through all the data. As stated in the previous round of review, computing the residuals and testing for additional controls is a recommended step in regression analysis and is performed after the initial step of obtaining the regression formula. What I am doing is not an alternative to regression but a recommended part of it.

Q: “Please add an explanation similar to “To compare this metric with soil production, Pelletier calculates P0 from every data point by regressing the soil production function, using a slope of h0 previously regressed in the Heimsath et al paper, to its h = 0 intercept.”

A: I prefer to leave the explanation as it is, since I am confused by what is meant by “regressing a function to its intercept.”

Q: “Eq. 2: why not write it with conventional units (cm) to comfort the reader i.e.:  $Pr = Pe^{0.031h}$ ”

A: Writing it in the way the reviewer suggests would involve units of  $\text{cm}^{-1}$ , not cm. I have a preference for defining scale parameters in terms of units of length or time rather than their inverse (e.g.,  $\exp(-h/h_0)$  rather than  $\exp(-\alpha h)$ ) because I think it is easier to understand length or time units. Of course if the reviewer or AE insists on this change I will make it.

Q: “I guess the author has reasons for it, but I am wondering why he is not plotting all the Heimsath data, calculate one soil production function from it, and use the thereby derived  $h_0$  value for the remaining part of his analysis. Actually, by using the two  $h_0$  values for  $Sav < 30$  and  $Sav > 30$  as derived by Heimsath et al., an a priori assumption is already made that weathering is higher for steeper regions. Isn't it the main goal of this paper to illustrate this using the residual values and could this point not be made stronger using a single soil production function and the therefrom derived  $h_0$  value? It is indeed remarkable that the 0-soil depth samples were excluded from the regressions presented in the Heimsath 2012 work. Including them and redrawing the SP function for  $S > 30$  shows more or less no trend raising the relevant question whether the data of SGM even support the exponential soil production function at  $S > 30^\circ$ . Therefore, I find it remarkable that the author uses the  $h_0$  value derived from the SPR function of this  $S > 30^\circ$  observations. A question which couples back to my previous remark.”

A: I don't see how using two different  $h_0$  values for  $Sav < 30$  and  $Sav > 30$  necessarily implies that weathering is higher for steeper regions. First, the two  $h_0$  values differ by only about 10%. Second,  $h_0$  values define how quickly soil production rates fall off with increasing soil thickness – they do not define the absolute values of soil production rates (these are set by  $P_0$  or  $Pr$ ).

I disagree with the reviewer's contention that plotting all of the data for  $Sav > 30$  reveals no trend. The data exhibit a hump, with the means of the clusters with  $h=0$  and  $h > 15$  cm lower than the cluster with  $0 < h < 15$ . Treating the data with  $h=0$  separately allows (but does not require) a humped production function. It would be OK to consider all of the data at once, but given that the data exhibit a hump it would only be acceptable to do this if one were to consider a mathematical formula consistent with a humped production function. Absent any general agreement on the mathematical form that governs the humped production function, I think fitting the data points with  $h > 0$  separately from those with  $h=0$  is the most defensible approach.

Q: “Page 5, line 3: should be  $1.78Pr$ , I guess...”

A:  $1.78P$  is correct as stated. As with the previous round of review, I do not understand why reviewers would suggest that I write  $Pr = 1.78Pr$ , which is mathematical nonsense.

Q: “Overall, it is not very clear to me how exactly  $Sav$  is calculated and whether  $Sav$  used in the equations (eg. Eq. 2 versus Eq. 3) is rather “ $Sav$  is defined by Heimsath et al. (2012) as the average slope over hillslopes adjacent to each sample location.” as mentioned on page 4 or “expressed in terms of the average slope from the drainage divide to the location of maximum slope rather than the shape parameter  $b/a$  used by Savage and Swolfs (1986). “ as mentioned on page 5.”

A: See responses to AE and other reviewers on this point.

Q: “Page 5, Line 23: Why not inserting the equation of Savage and Swolfs (1986) in your text? That would increase overall readability of the paper.”

A: Done. Added: “Savage and Swolfs (1986) studied role of topography in modifying local stresses in a model ridge and valley geometry that uses a conformal transformation that includes length scales  $b$  and  $a$  that define the vertical and horizontal extents of the ridge, respectively. Because the data from Heimsath et al. (2012) are acquired from locations at or near ridgetops, I focused only on the portion of the Savage and Swolfs (1986) solution between the ridgetop and the point of maximum slope, i.e., the broad, U-shaped valley bottoms flanking the central ridge were not considered. The average slope,  $S_{av}$ , computed from between the ridgetop and the point of maximum slope, is equal to  $b/4a$  in the mathematical framework of Savage and Swolfs (1986). A key result of Savage and Swolfs (1986) is their prediction of a gradual decline in the horizontal compressive stress near ridgetops as  $b/a$  increases between 0 and 2 (their Figure 4) based on their equation (36):

$$\frac{\sigma_{xx}}{N_1} = \frac{2-b/a}{(2+b/a)(1+b/a)} \quad (3)$$

where  $N_1$  is the regional maximum compressive stress and  $S_{av}$  has units of m/m in equation (3). Substituting  $4S_{av}$  for  $b/a$  in equation (3) yields:

$$\frac{\sigma_{xx}}{N_1} = \frac{2-4S_{av}}{(2+4S_{av})(1+4S_{av})} \quad (4)$$

Note that the tangent of the slope angle (units of m/m) is averaged to obtain  $S_{av}$  in all cases in this paper. However, after this averaging,  $S_{av}$  is reported in degrees in some cases to facilitate comparison with the results of Heimsath et al. (2012).”

Q: “Page 6, Line3: “Gravitational stresses can be included”, are they also included in the analysis? If not I suggest leaving the following paragraph out or at least summarizing it.”

A: I added an explicit statement that gravitational stresses are not included. I think it is crucial that I include at least a quantitative discussion of how including gravitational stresses would modify the results, which is what the following paragraph does. I agree that this paragraph is somewhat dense and technical, but I feel strongly that this discussion is necessary.

Q: “Eq. 4, it could be helpful for the readers to color the different line segments of Fig. 2 as calculated under the three conditions.”

A: I have added text in the caption to make this point: “The piece-wise curve plots equation (5), with the three segments of the curve corresponding to the three conditions in the equation.”

Q: “If I understand the procedure correctly, I am afraid that I do not support the way in which the  $z > 2300$  m data points are being treated and I feel this is an issue which should be resolved (or better explained in case I misunderstand this). Eq. 4 (Pr) is calculated excluding the  $>2300$  m data points. Next, the same Pr values are used to compare the  $>2300$  m points from the  $<2300$  points. Of course, there is a difference in the mean value of the difference between the predicted Pr value and the data points of the  $z > 2300$  points because they were not included when calculating Pr. This procedure makes no sense as such. Maybe a simple variance analysis could do the trick?”

A: The reviewer is obviously correct that the means of any two populations will not be precisely identical. However, a t test for unequal means tests whether or not two populations are sampled from *statistically distinct sets* as measured by the similarity of their mean values and taking into account the variances within each population. Two populations can certainly have (and always will have) means that are not precisely identical, but the test I employed determines whether or not the two populations represent statistically distinct sets (for example, comparing rolls of the dice between two sets of dice, one of which might be loaded or biased). To address this issue I have reworded the sentence: “**Assuming a significance level of 0.05, the null hypothesis that the cluster of blue points is sampled from the same statistical set as that of the remaining points with Sav > 30° (i.e., that both sets are governed by the same process or controlling variables) can be rejected based on the standard t test with unequal variances (t = 0.021).**”

Q: “*Because of my previous remark, I feel troubled with Eq. 5. If temperature and vegetation cover is indeed controlling weathering rates as proposed by Pelletier, why not including a temperature factor or vegetation factor directly into Eq. 5 rather than using a discrete proxy for climate. Has the author tested such approach? I find too much weight is now given to a so called cluster of only 4 residual points in order to prove the importance of climate.*”

A: I worked hard to include a vegetation factor into the analysis but in the end I could not find a definitive answer. Primarily this is because vegetation cover depends on the recent fire history of a mountain range (areas that have burned recently have vegetation cover unrelated to temperature and precipitation) in addition to factors such as temperature and precipitation. Moreover, there are many ways of quantifying vegetation (via type, canopy height, above-ground biomass, etc.) and each gives somewhat different answers. As for temperature, the only spatially distributed temperature data available for the SGM are interpolations (such as PRISM or WorldClim) that are based almost entirely on elevation-based regressions. As such, I think it is more straightforward and honest to use elevation directly as a controlling variable rather than a modeled variable (temperature) that is based heavily on elevation.

Q: “*Of the entire paper, I find this section least convincing. Here the author stretches his empirical findings to the limit, based on some questionable assumptions (eg. assuming a steady state between uplift and erosion is far less evident than often assumed (Mudd, 2016)) and a weak correlation between soil depth and Sav. I see what the author tries to do in Figure 7 but find a visual comparison and evaluation of the obtained results not a good evidence for the proposed theory. I would find a simple model exercise, at a 2D profile or a landscape scale, very helpful here (e.g. with one of the many LEMs the author developed in previous work). In such an exercise the author could investigate whether or not, the adapted soil production rates, depending on topographically induced stress, does indeed allow to reproduce increasing weathering rates with simultaneously increasing erosion rates (without direct control of erosion on weathering rates). If such a trend could be observed, this would indeed offer a valid and alternative theory to explain the observation of Heimsath 2012 that weathering rates increase with increasing erosion rates. If the author wants to keep his current approach, I strongly recommend some more quantitative approaches to interpret the findings. Of special interest could be a plot comparing predicted erosion rates with measured catchment wide denudation rates (which are available for this region: Dibiase, 2010).*”

A: Please note that the steady state I assumed in section 2.2 is a soil thickness steady state, not a topographic steady state as the reviewer states. In fact, I made a special point of noting that the modeling in section 2.2 makes no assumption regarding uplift rates. A soil-thickness steady state condition is assumed in all *in situ* CRN calculations and is likely to be more widely applicable than a topographic steady state (see Heimsath et al., 2002 for a discussion).

Section 2.2 is useful because it demonstrates how the various correlations identified using individual data points plays out across the landscape at larger spatial scales. I think there is value in this. Moreover, this section demonstrates the role that soil thickness plays, which is not explicitly considered in Section 2.1. Soils always tend to thin in areas of steeper slopes, thereby allowing the soil production rate to increase in concert with the erosion rate. Now that Heimsath et al. (2012) have demonstrated that in the SGM potential soil production rates also increase with slope, this begs the question of whether (or how much) soils still thin as slope steepens. The analysis of Section 2.2. demonstrates that this type of thinning still occurs, just not to the extent that it would were it not for the positive correlation between  $P_r$  values and average slope.

In the revision I have compared the model-based erosion rates with CRN-based catchment-averaged erosion rates. I thank the reviewer for this excellent suggestion. The added text is as follows:

“The model can be further tested by comparison to the catchment-averaged erosion rates reported by DiBiase et al. (2010). Figure 8 plots catchment-averaged erosion rates (unfilled circles) as a function of catchment-averaged  $S_{av}$  values. As with the  $P_r$  values plotted in Figure 2C, I averaged the data in bins of slope in order to minimize local variability related to factors besides average slope. The solid curve represents the model prediction for erosion rate, i.e., equation (8) with  $P_r$  values predicted by equation (5) and  $h$  values predicted by equation (10). Catchment-averaged erosion rates follow a similar pattern as predicted values, remaining constant or increasing slightly with increasing  $S_{av}$  until  $S_{av} \approx 30^\circ$ , beyond which erosion rates increase abruptly. The similarity between  $E$  and  $P_r$  values (Figs. 8 and 2) reflects the important influence of  $S_{av}$  on both variables, the coupling between these variables (i.e., in the absence of widespread landsliding in bedrock or intact regolith, soil must be produced in order for erosion to occur), and the modest impact that differences in soil thickness have on soil production rates across landscapes of different relief in the SGM. Except for several data points of relatively high erosion rates at both the lowest ( $S_{av} = 10\text{-}15^\circ$ ) and highest slopes ( $S_{av} > 35^\circ$ ), the model reproduces the absolute values and the slope dependence of the measured erosion rates reasonably well. The underprediction of the model at the highest slopes may be due, in part, to the fact that the  $P_r$  values used to calibrate the model has relatively few data points near the highest end. For example, 4 of 57  $P_r$  values are above 500 m/Myr, while 11 of 50 catchments have erosion rates above this value. The comparison of the predicted curve to the model is not meant to imply that the model prediction is the best or only mathematical expression that represents the data. Rather, Figure 8 (and Figure 2 for the model-data comparison of  $P_r$  values) is intended only to demonstrate consistency with the threshold increase at  $S_{av} \approx 30^\circ$  predicted by the Savage and Swolfs (1986) model.

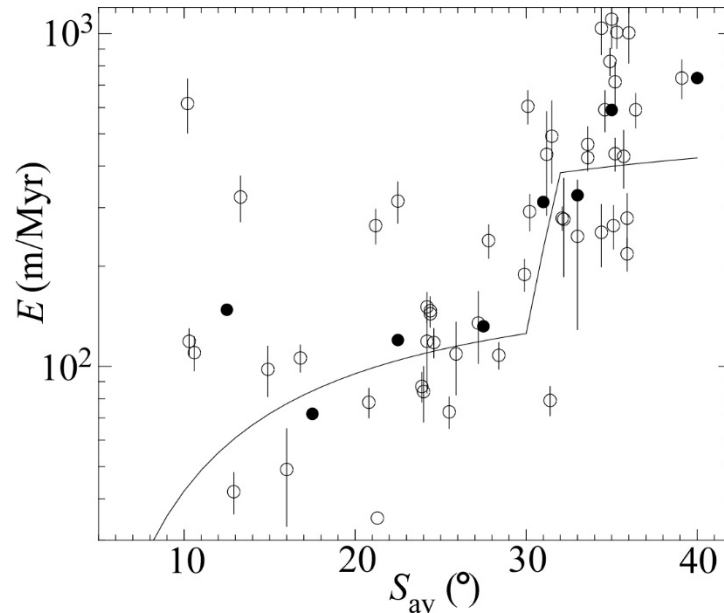


Figure 8. Plot of the catchment-averaged erosion rates of DiBiase et al. (2010) (unfilled circles) versus catchment-averaged  $S_{av}$ . Filled circles represent log-transformed averages of data within the following bins: 10-15°, 15-20°, 20-25°, 25-30°, 30-32°, 32-34°, and 34-36°. The curve plots the model prediction, i.e., equation (8) with  $P_r$  values predicted by eqn. (5) and  $h$  values predicted by equation (10).”

## Quantifying the controls on potential soil production rates: A case study of the San Gabriel Mountains, California

Jon D. Pelletier

Department of Geosciences, University of Arizona, Gould-Simpson Building, 1040 East Fourth Street, Tucson, Arizona 85721-0077, USA

Correspondence to: Jon D. Pelletier (jdpellet@email.arizona.edu)

**Abstract.** The potential soil production rate, i.e., the upper limit at which bedrock can be converted into transportable material, limits how fast erosion can occur in mountain ranges in the absence of widespread landsliding in bedrock or intact regolith. Traditionally, the potential soil production rate has been considered to be solely dependent on climate and rock characteristics. Data from the San Gabriel Mountains of California, however, suggest that topographic steepness may also influence potential soil production rates. In this paper I test the hypothesis that topographically induced stress opening of pre-existing fractures in the bedrock or intact regolith beneath hillslopes of the San Gabriel Mountains increases potential soil production rates in steep portions of the range. A mathematical model for this process predicts a relationship between potential soil production rates and average slope consistent with published data. Once the effects of average slope are accounted for, evidence a small subset of the data suggest that temperature limits cold temperatures may limit soil production rates at the highest elevations of the range can also be detected due to the influence of temperature on vegetation growth. These results confirms suggest that climate and rock characteristics control may be the sole controls on

potential soil production rates as traditionally assumed, but that the porosity of bedrock or intact regolith ~~can~~may evolve with topographic steepness in a way that enhances the persistence of soil cover in compressive-stress environments. I develop an empirical equation that relates potential soil production rates in the San Gabriel Mountains to the average slope and a climatic index that accounts for temperature limitations on soil production rates at high elevations. Assuming a balance between soil production and erosion rates at the hillslope scale, I illustrate the interrelationships among potential soil production rates, soil thickness, erosion rates, and topographic steepness that result from the feedbacks among geomorphic, geophysical, and pedogenic processes in the San Gabriel Mountains.

*Keywords: soil production, cosmogenic radionuclides, topographically induced stress, San Gabriel Mountains*

## 1 Introduction

The potential soil production rate (denoted herein by  $P_r$ ) is the highest rate, achieved when soil cover is thin or absent, that bedrock or intact regolith can be converted into transportable material at each point on Earth's surface.  $P_r$  values are the rate-limiting step for erosion in areas where landsliding in bedrock or intact regolith is not widespread, because soil must be produced before it can be eroded. Slope ~~failure~~failures in bedrock or intact regolith ~~is~~are common in some fine-grained sedimentary rocks (e.g., Griffiths et al., 2004; Roering et al., 2005) but ~~relatively uncommon in granitic rock types.~~may be less common in massive lithologies such as granite.

Despite its fundamental importance, the geomorphic community has no widely accepted conceptual or mathematical model for potential soil production rates. Pelletier and Rasmussen (2009) took an initial step towards developing such a model by relating  $P_r$  values in granitic landscapes to mean annual precipitation and temperature values. The goal of ~~this~~that model was to quantify how water availability and vegetation cover control the potential soil production rate across the extremes of Earth's climate. The Pelletier and Rasmussen (2009) model predicts  $P_r$  values consistent with those reported in the literature from semi-arid climates, where  $P_r$  values typically range from ~30-300 m/Myr. In humid climates, the Pelletier and Rasmussen (2009) model predicts  $P_r$  values greater than 1000 m/Myr (Fig. 2A of Pelletier and Rasmussen, 2009). This is broadly consistent with measured soil production rates ~~of up~~

~~to 2500 m/Myr~~ in the Southern Alps of New Zealand where the mean annual precipitation (MAP) exceeds 10 m (Larsen et al., 2014). The Pelletier and Rasmussen (2009) model was a useful first step, but clearly not all granites are the same. In particular, variations in mineralogy (Hahm et al., 2014) and bedrock fracture density (Goodfellow et al., 2014) can result in large variations in soil production rates in granites within the same climate.

The San Gabriel Mountains (SGM) of California (Fig. 1) have been the focus of many studies of the relationships among tectonic uplift rates, climate, geology, topography, and erosion (e.g., Lifton and Chase, 1992; Spotila et al., 2002; DiBiase et al., 2010; 2012; DiBiase and Whipple, 2011; Heimsath et al., 2012; Dixon et al., 2012). These studies take advantage of a significant west-to-east gradient in exhumation rates in this range. Spotila et al. (2002) documented close associations among exhumation rates, mean annual precipitation (MAP) rates, and the locations and densities of active tectonic structures. Mean annual precipitation (MAP) rates vary by a factor of two across the elevation gradient and exhibit a strong correlation with exhumation rates (Spotila et al., 2002, their Fig. 10). Lithology, which varies substantially across the range (Fig. 1), also controls exhumation rates. Spotila et al. (2002) demonstrated that exhumation rates are lower, on average, in rocks relatively resistant to weathering (i.e., granite, gabbro, anorthosite, and intrusive rocks) compared to the less resistant schists and gneisses of the range (Spotila et al., 2002, their Fig. 9). This lithologic control on long-term erosion rates can control drainage evolution. For example, Spotila et al. (2002) concluded that the San Gabriel River has exploited the weak Pelona Schist to form a rugged canyon between ridges capped by more resistant Cretaceous granodiorite (e.g., Mount Baden Powell). Spotila et al. (2002) concluded that landscape evolution in the SGM was controlled by a combination of tectonics, climate, and rock characteristics.

Heimsath et al. (2012) provided a millennial-time-scale perspective on the geomorphic evolution of the SGM. These authors demonstrated that soil production rates ( $P$ ) and erosion rates ( $E$ ) in rapidly eroding portions of the SGM greatly exceed  $P_r$  values in slowly eroding portions of the range. Heimsath et al. (2012) concluded that high erosion rates, triggered by high tectonic uplift rates and the resulting steep topography, cause potential soil production rates to increase above any limit set by climate and bedrock characteristics. Their results challenge the traditional view that  $P_r$  values are controlled solely by climate and rock characteristics.

Recent research, stimulated by shallow seismic refraction and drilling campaigns, has documented the importance of topographically induced stresses on the development of new fractures (and the opening of pre-existing fractures) in bedrock or intact regolith beneath hillslopes and valleys (e.g. Miller and Dunne, 1996; Martel, 2006; 2011; Slim et al., 2014; St. Clair et al., 2015). In this process, the bulk porosity of bedrock and intact regolith evolves with topographic ruggedness (i.e., topographic slope ~~and~~ or curvature). In a compressive-stress environment such as the SGM, topographically induced stresses can result in lower compressive stresses, or even tensile stresses, in rocks beneath hillslopes near ridgetops. As an elastic solid is compressed, surface rocks undergo outer-arc stretching where the surface is convex-outward (i.e., on hillslopes), reducing the horizontal compressive stress near the surface and eventually inducing tensile stress near ridgetops in areas of sufficient ruggedness. Such stresses can generate new fractures or open pre-existing fractures in the bedrock or intact regolith, allowing potential soil production rates to increase. In this paper I test whether potential soil production rates estimated using the data of Heimsath et al. (2012) are consistent with the topographically induced stress fracture opening hypothesis in the SGM. This hypothesis predicts a relationship between  $P_r$  values and average slope that is consistent with the data of Heimsath et al. (2012). Once the effects of average slope are accounted for, I test the hypotheses that climate, lithology, and local fault density also influence  $P_r$  values. I then use the resulting empirical model for  $P_r$  values to map the spatial variations in potential soil production rates, soil thickness, erosion rates, and topographic steepness across the range in order to illustrate the interrelationships among these variables.

## 2 Data analysis and mathematical modeling

### 2.1 Controls on potential soil production rates in the SGM

Estimates of the maximum or potential soil production rate (i.e., the soil production rate obtained when the buffering effects of soil, if present, are factored out of the measured soil production rate) for the SGM can be estimated using the residuals obtained from the regression of soil production rates to soil thicknesses reported by Heimsath et al. (2012) (their Fig. 3). The exponential form of the soil production function quantifies the decrease in soil production rates with increasing soil thickness:

$$P = P_r e^{-h/h_0}, \quad (1)$$

where  $h$  is soil thickness and  $h_0$  is a length scale quantifying the relative decrease in soil production rates for each unit increase in soil thickness. Regressing their data to equation (1), Heimsath et al. (2012) obtained  $h_0 = 0.32$  m for locations with an average slope,  $S_{av}$ , ~~of~~ less than or equal to  $30^\circ$  and  $h_0 = 0.37$  m for locations with  $S_{av} > 30^\circ$ .  ~~$S_{av}$  is defined by Heimsath et al. (2012) as the average slope over hillslopes adjacent to each sample location.~~ Values of the maximum potential soil production rate (Supplementary Table 1) can be estimated as the residuals obtained by dividing the  $P$  values measured by Heimsath et al. (2012) by the exponential term in equation (1):

$$P_r = \begin{cases} P e^{h/0.32 \text{ m}} & \text{if } S_{av} \leq 30^\circ \\ P e^{h/0.37 \text{ m}} & \text{if } S_{av} > 30^\circ \end{cases} \quad (2)$$

Note that equation (2) is equivalent to subtracting the logarithms of the exponential term from the logarithms of  $P$  values, since division is equivalent to subtraction under log transformation. Log transformation is appropriate in this case because  $P$  values are positive and positively skewed (i.e., there are many  $P$  values in the range of 50–200 m/Myr and a smaller number of values in the range of 200–600 m/Myr that would be heavily weighted in the analysis if the data were not log-transformed).  $P_r$  values estimated from equation (2) increase, on average, slowly with increasing  $S_{av}$  (Fig. until 2A).  $P_r$  values exhibit an abrupt increase at an  $S_{av}$  of approximately  $30^\circ$  (Fig. 2A).

Heimsath et al. (2012) did not include data points from locations without soil cover in their regressions because these data points appear (especially for areas with  $S_{av} > 30^\circ$ ) to fit below the trend of equation (1). This implies that a humped production function may be at work in some portions of the SGM. The mean value of  $P$  from areas with  $S_{av} \leq 30^\circ$  that lack soil cover is 183 m/Myr, i.e., slightly higher than, but within  $2\sigma$  uncertainty of, the  $170 \pm 10$  m/Myr value expected based on the exponential soil production function fit by Heimsath et al. (2012). As such, the evidence indicates that for areas with  $S_{av} \leq 30^\circ$ , data from locations with and without soil cover are both consistent with an exponential soil production function. The mean value of  $P$  from areas with  $S_{av} > 30^\circ$  that lack soil cover is 207 m/Myr, i.e., significantly lower than the  $370 \pm 40$  m/Myr expected based on the exponential soil production

function. This suggests that a hump may exist in the soil production function for steep ( $S_{av} > 30^\circ$ ) slopes as they transition to a bare (no soil cover) condition. To account for this, I estimated  $P_r$  to be equal to  $1.78P$  (i.e., the ratio of 370 to 207) at locations with  $S_{av} > 30^\circ$  that lack soil cover.

The SGM has horizontal compressive stresses of  $\sim 10$  MPa in an approximately N-S direction at depths of less than a few hundred meters (e.g., Sbar et al., 1979; Zoback et al., 1980; Yang and Hauksson, 2013). The development of rugged topography can lead to topographically induced fracturing of bedrock ~~and/or~~ opening of pre-existing fractures near ridgetops in compressive-stress environments (e.g., Miller and Dunne, 1996; Martel, 2006; Slim et al., 2014; St. Clair et al., 2015). Given the pervasively fractured nature of bedrock in the SGM (e.g., Dibiase et al., 2015), I assume that changes in the stress state of bedrock or intact regolith beneath hillslopes near ridgetops leads to the opening of pre-existing fractures (i.e., an increase in the bulk porosity of bedrock or intact regolith) rather than the fracturing of intact rock. I adopt the analytic solutions of Savage and Swolfs (1986), who solved for the topographic modification of regional compressive stresses beneath ridges and valleys oriented perpendicular to the most compressive stress direction. Savage and Swolfs (1986) demonstrated that the horizontal stress ( $\sigma_{xx}$ ) in bedrock or intact regolith becomes less compressive under ridges as the slope increases (Fig. 3). In landscapes with a maximum slope larger than  $45^\circ$  (equivalent to an average slope of approximately  $27^\circ$  or  $\tan(0.5)$  in the mathematical framework of Savage and Swolfs, 1986), bedrock or intact regolith that would otherwise be in compression develops tensile stresses close to the surface beneath hillslopes (Fig. 3A). An average slope of  $27^\circ$  is close to the threshold value of  $30^\circ$  that Heimsath et al. (2012) identified as representing the transition from low to high  $P_c$  values in the SGM. Therefore, the abrupt increase in  $P_r$  values at approximately  $30^\circ$  is consistent with a transition from compression to tension in bedrock or intact regolith beneath hillslopes of the SGM. In addition to this sign change in the horizontal stress state in the rocks beneath hillslopes of the SGM, the Savage and Swolfs (1986) model predicts a gradual decline in horizontal compressive stress as  $S_{av}$  increases between 0 and approximately  $27^\circ$  (Fig. 3B); near

ridgetops as the average slope (measured over a spatial scale that includes ridgetops and side slopes) increases (Fig. 3).

Savage and Swolfs (1986) studied the role of topography in modifying local stresses in a model ridge-and-valley geometry that uses a conformal transformation that includes length scales  $b$  and  $a$  that define the vertical and horizontal extents of the ridge, respectively. Because the data from Heimsath et al. (2012) are acquired from locations at or near ridgetops, I focused only on the portion of the Savage and Swolfs (1986) solution between the ridgetop and the point of maximum slope, i.e., the broad, U-shaped valley bottoms flanking the central ridge were not considered. The average slope,  $S_{av}$ , computed from between the ridgetop and the point of maximum slope, is equal to  $b/4a$  in the mathematical framework of Savage and Swolfs (1986). A key result of Savage and Swolfs (1986) is their prediction of a gradual decline in the horizontal compressive stress near ridgetops as  $b/a$  increases between 0 and 2 (their Figure 4) based on their equation (36):

$$\frac{\sigma_{xx}}{N_1} = \frac{2-b/a}{(2+b/a)(1+b/a)} \quad (3)$$

~~$$\frac{\sigma_{xx}}{N_1} = \frac{2-4S_{av}}{(2+4S_{av})(1+4S_{av})} \quad (3)$$~~

where  $N_1$  is the regional maximum compressive stress and  $S_{av}$  has units of m/m in equation (3).

Substituting  $4S_{av}$  for  $b/a$  in equation (3) is simply equation (36) of Savage and Swolfs (1986) expressed in terms of the average slope from the drainage divide to the location of maximum slope rather than the shape parameter  $b/a$  used by Savage and Swolfs (1986). yields:

~~$$\frac{\sigma_{xx}}{N_1} = \frac{2-4S_{av}}{(2+4S_{av})(1+4S_{av})} \quad (4)$$~~

Note that the tangent of the slope angle (units of m/m) is averaged to obtain  $S_{av}$  in all cases in this paper.

However, after this averaging,  $S_{av}$  is reported in degrees in some cases to facilitate comparison with the results of Heimsath et al. (2012).

In landscapes with  $S_{av} > 27^\circ$  or  $\text{atan}(0.5)$ , bedrock or intact regolith that would otherwise be in compression develops tensile stresses close to the surface near ridgetops (Fig. 3A). An average slope of  $27^\circ$  is close to the threshold value of  $30^\circ$  that represents the transition from low to high  $P_r$  values in the SGM (Fig. 2). Therefore, the abrupt increase in  $P_r$  values at  $S_{av} \approx 30^\circ$  is consistent with a transition from compressive to tensile stresses in bedrock or intact regolith near ridgetops of the SGM.

The average slope computed from the model geometry is consistent with the average slope computed by Heimsath et al. (2012). The average slope in the model is computed from the ridgetop to the point of maximum slope in the model geometry. In the SGM, as with any region of narrow, V-shaped valleys, the steepest portion of the hillslope tends to occur at or near the slope base. Heimsath et al. (2012) computed their average slope from hillslope patches (valley bottoms were excluded) over a length scale that included ridgetops and side slopes. As such, the two calculations are consistent.

It is important to note that the local stress modification in the Savage and Swolfs (1986) model is a function of both local curvature and the slope averaged over a spatial scale that includes ridgetops and side slopes. Within an individual hillslope, local curvature controls the sign of stress modification, with a reduction in compressive stress (and development of tensile stress in sufficiently rugged terrain) occurring beneath ridgetops and an increase in compressive stress occurring beneath valley bottoms. The compressive-stress reduction that occurs beneath ridgetops is the most important response of the model for the purposes of this paper since the  $P_r$  data are from locations at or near ridgetops (i.e., 24 of the 57 data points are on ridgetops, with the remaining data points located within approximately 100 m from ridgetops). The magnitude of the extension near ridgetops is controlled by the landscape-scale slope, quantified by Savage and Swolfs (1986) as  $b/a$ . Since  $b$  and  $a$  are length scales that define the vertical and horizontal extents of the ridge rather than the slope at any one location, the average slope computed over a length scale that includes ridgetops and side slopes is the variable most consistent with  $b/a$ .

Figure 3 illustrates the effects of topography on tectonic stresses only, i.e., gravitational stresses are not included. Gravitational stresses can be included in the model by superposing the analytic solutions

of Savage and Swolfs (1986) (their equations (34) and (35)) with the solutions of Savage et al. (1985) ~~for that quantify~~ the effects of topography on gravitational stresses (their equations (39) and (40)). The result ~~is would be~~ a three-dimensional phase space of solutions corresponding to different values of the regional tectonic stress  $N_1$ , the characteristic gravitational stress  $\rho gb$  (where  $\rho$  is the density of rock,  $g$  is the acceleration due to gravity, and  $b$  is the ridge height), and the Poisson ratio  $\mu$ . Qualitatively, the effects of ~~including~~ gravitational stresses ~~are would be~~ 1) to increase the compression at depth via the lithostatic term (at soil depths this corresponds to an addition of  $\sim 10$  kPa, which is negligible compared to the regional compressive stress of  $\sim 10$  MPa in the SGM), and 2) to increase the compressive stresses near the point of inflection on hillslopes (e.g., Fig. 2a of Savage et al., 1985). These modifications do not alter the first-order behavior illustrated in Figure 3 for ~~rocks close to the surface that are not close to hollows or other points of inflection.~~ Locations near ridgetops. Section 3 provides additional discussion of the assumptions and alternative approaches to modeling topographically induced stresses.

The fit of the solid curve in Figure 2A to  $P_r$  values is based on equation (34), together with an assumption that the transition from compressive to tensile stresses triggers a step increase in  $P_r$  values over a small range of  $S_{av}$  values in the vicinity of the transition from compression to tension:

$$P_{r,S} = \begin{cases} P_{r,l} \left(1 - \frac{\sigma_{xx}}{N_1}\right) & \text{if } S_{av} \leq S_l \\ P_{r,h} \left(1 - \frac{\sigma_{xx}}{N_1}\right) & \text{if } S_{av} > S_h \\ \left(P_{r,l} + (P_{r,h} - P_{r,l}) \frac{S_{av} - S_l}{S_h - S_l}\right) \left(1 - \frac{\sigma_{xx}}{N_1}\right) & \text{if } S_l \leq S_{av} < S_h \end{cases}$$

(45)

where  $P_{r,S}$  denotes the model for the dependence of  $P_r$  values on  $S_{av}$ ,  $P_{r,l}$  and  $P_{r,h}$  are coefficients defining the low and high values of  $P_r$ , and  $S_l$  and  $S_h$  are the average slopes defining the range over which  $P_r$  values increase from low to high values across the transition from compression to tension.  $P_{r,l}$  and  $P_{r,h}$  were determined to be 170 m/Myr and 500 m/Myr based on least-squares minimization to the data (data from elevations above 2300 m were excluded because of the climatic influence described below).  $S_l$  and  $S_h$

were chosen to be  $30^\circ$  and  $32^\circ$ , respectively, to characterize the abrupt increase in  $P_r$  values in the vicinity of  $30^\circ$ . The null hypothesis that  $P_{r,s}$  values can be fit as well or better by a linear relationship can be rejected: the reduced- $\chi^2$  value, which takes into account different numbers of degrees of freedom, of the log-transformed values of equation (5), is less than half (45%) of the reduced- $\chi^2$  for a least-squares linear fit. It should be noted that there is effectively no theory or model prediction for how  $P_r$  values increase above the abrupt increase in values at  $S_{av} \approx 30^\circ$ . Equation (5) makes the parsimonious assumption that  $P_r$  values continue to increase proportionally to  $1-\sigma_{xx}/N_1$  above the abrupt increase at  $S_{av} \approx 30^\circ$ . More sophisticated models would be required to make a more informed prediction regarding how weathering rates might be modified by an increasing magnitude of tensile stress.

In addition to the average slope control associated with the topographically induced stress fracture opening process, a climatic control on  $P_r$  values ~~can be identified using~~ is suggested by the results of a cluster analysis. This type of analysis involves identifying clusters in the data ~~defined by distinctive~~ that are sampled from distinct sets or processes based on the dissimilarity of the means values of the ~~independent variables that also have different mean values of the dependent variable~~ clusters, taking into account the variation within each cluster. The four points colored in blue in Figure 2A are the four highest elevation samples in the dataset, with elevations  $\geq 2300$  m a.s.l. The logarithms (base 10) of this cluster have a mean value of -0.40 after subtracting the logarithms of  $P_{r,s}$  to account for the average slope control on  $P_r$  values, compared with a mean of 0.00 for the logarithms of the remaining data points with  $S_{av} > 30^\circ$  (also with the logarithms of  $P_r$  subtracted). Assuming a significance level of 0.05, the null hypothesis that the cluster of blue points ~~has a mean that is indistinguishable~~ sampled from the same set as that of the remaining points with  $S_{av} > 30^\circ$  (i.e., that both sets are governed by the same process or controlling variables) can be rejected based on the standard t test with unequal variances ( $t = 0.021$ ).

Figures 4A-4C illustrate the mean annual temperature (MAT), mean annual precipitation (MAP), and existing vegetation height (EVH) for the central portion of the SGM. Above elevations of approximately 1800 m a.s.l., vegetation height decreases systematically with increasing elevation (Fig.

4D). This limitation is likely to be primarily a result of temperature limitations on vegetation growth because MAP increases with elevation up to and including the highest elevations of the range. ~~This result is consistent with the hypothesis that vegetation is a key driver of soil production. The decrease in  $P_0$  values with elevation is likely to be gradual rather than abrupt, and indeed there is evidence of a peak in the climatic control of  $P_0$  values.~~ Figure 4E plots the ratio of  $P_r$  to  $P_{r,s}$  as a function of elevation. The closed circles are binned averages of the data (each bin equals 100 m in elevation). The ratio of  $P_r$  to  $P_{r,s}$  (equivalent to the residuals under log transformation after the effects of average slope are removed) increases, on average, and then decreases within the range of elevations between 1500 and 2600 m, broadly similar to the trend of EVH (Fig. 4D). Some differences between the curves are to be expected due to the fact that EVH is influenced by the recent fire history, which temporarily reduces EHV in locations that have experienced fire in recent decades. Despite that complication, the fact that both EHV and  $P_r/P_{r,s}$  exhibit broadly similar increases and then decreases suggests a causal connection between vegetation cover and weathering rates consistent with a temperature/vegetation limitation on  $P_r$  values at the highest elevations of the SGM.

Local variability in  $P_r$  estimates due to variations in soil thickness, mineralogical variations within a given lithology, spatial variations in fracture density, etc. can be minimized by averaging  $P_r$  values (not including the four highest-elevation points because of the climatic control) from locations that have the same average slope (Fig. 2C). This process tends to average data from the same local cluster since local clusters often have average slopes that are both equal within the cluster and different from other clusters. Figure 2C demonstrates that the predictions of the topographically induced stress fracture opening hypothesis are consistent with the observed dependence of  $P_r$  values on  $S_{av}$  values.

The average slope and climatic controls on  $P_r$  values can be combined into a single predictive equation for  $P_r$  values:

$$P_{r,\text{pred}} = P_{r,s}C \quad (56)$$

where  $P_{r,\text{pred}}$  denotes predicted values for  $P_r$ ,  $C$  is a climatic index defined as 1 for  $z < 2300$  m and 0.4 (i.e., the ratio of the mean of the logarithms of the data for  $z > 2300$  m to the mean of the logarithms of remaining data points with  $S_{\text{av}} > 30^\circ$ ) for  $z > 2300$  m. A regression of  $P_{r,\text{pred}}$  values to  $P_r$  values yields an  $R^2$  of 0.50 (Fig. 2D). When data with equal  $S_{\text{av}}$  values are averaged (i.e., the filled circles in Fig. 2D), the resulting  $R^2$  value is 0.87.

The results of this section demonstrate that average slope and possibly climate exert controls on  $P_0$  $P_r$  values in the SGM. Although I did not find additional controls that were clearly distinct from these, it is worth discussing additional controls that I tested for. The data points colored in gray in Figure 2B are from the three rock types most resistant to weathering as determined by Spotila et al. (2002): granite, anorthosite, and the Mount Lowe intrusive suite. Spotila et al. (2002) also identified gabbro as a relatively resistant rock in the SGM, but no soil production rates are available from this rock type. Figure 2B suggests that lithology might exert some control on  $P_r$  values. Specifically, 7 samples from the more resistant lithologies sit above the least-squares fit of equation (4) to the data, while 13 (including the 7 lowest  $P_0$  values) sit below the least-squares fit. However, the null hypothesis that the residuals of the gray cluster (after the effects of average slope are removed) has a mean that is indistinguishable from the residuals of the remaining points (colored black in Figure 2B) cannot be rejected ( $t = 0.21$ ).

Many studies have proposed a relationship between fracture density and bedrock weatherability on the basis that fractures provide additional surface area for chemical weathering and pathways for physical weathering agents to penetrate into the bedrock or intact regolith (e.g., Molnar, 2004; Molnar et al., 2007; Goodfellow et al., 2014; Roy et al., 2016a,b). The difference in erosion rates between the SGM and adjacent San Bernadino Mountains, for example, has been attributed in part to differences in fracture density between these ranges (Lifton and Chase, 1992; Spotila et al., 2002). As such, it is reasonable to hypothesize that differences in  $P_r$  values might result from spatial variations in fracture density within each range. I computed a bedrock damage index  $D$  based on the concept that  $P_r$  values increase in bedrock that is more pervasively fractured, together with the fact that bedrock fracture densities are

correlated with local fault density in the SGM (Chester et al., 2005; Savage and Brodsky, 2011). Savage and Brodsky (2011) documented that bedrock fracture density decreases as a power-law function of distance from small isolated faults, i.e. as  $r^{-0.8}$  where  $r$  is the distance from the fault. Fracture densities around larger faults and faults surrounded by secondary fault networks can be modeled as a superposition of  $r^{-0.8}$  decays from all fault strands (Savage and Brodsky, 2011). Chester et al. (2005) documented similar power-law relationships between bedrock fracture density and local fault density in the SGM specifically. I define the bedrock damage index  $D$  (Fig. 5A) as the sum of the inverse distances, raised to an exponent 0.8, from the point where the  $D$  value is being computed to every pixel in the study area where a fault is located:

$$D = \sum_{\mathbf{x}'} \left( \Delta x / |\mathbf{x} - \mathbf{x}'| \right)^{0.8} \quad (6)$$

(7)

where  $\Delta x$  is the pixel width,  $\mathbf{x}$  is the map location where bedrock damage is being computed, and  $\mathbf{x}'$  is the location of each mapped pixel in SGM where a fault exists.  $D$  has units of length since it is the sum of all fault lengths in the vicinity of a point, weighted by a power function of inverse distance. Equation (6) honors the roles of both the distance to and the local density of faults documented by Savage and Brodsky (2011) because longer faults and/or more mature fault zones with many secondary faults have more pixels that contribute to the summation. The fact that a relationship exists between  $P_r$  values and  $D$  (Fig. 5B,  $p = 0.035$ ) and between  $D$  and  $S_{av}$  (Fig. 5C,  $p = 0.015$ ) suggests that some of the control by average slope that I have attributed to the topographically induced stress fracture opening process may reflect differences in the density of pre-existing fractures related to local fault density. However, the much higher  $R^2$  value of the relationship between  $P_r$  and  $P_{r,pred}$  ( $R^2 = 0.50$ ) compared to that for the relationship between  $P_r$  and  $D$  ( $R^2 = 0.08$ ) suggests that the topographically induced stress fracture opening process is the dominant mechanism controlling  $P_r$  values in the SGM. In addition, this process has a stronger theoretical foundation.

## 2.2 Relating potential soil production rates to erosion rates and topographic steepness in the SGM

In this section I invoke a balance between soil production and transport at the hillslope scale in order to illustrate the interrelationships among potential soil production rates, erosion rates, soil thicknesses, and average slopes spatially across the SGM. The conceptual model explored in this section is based on the hypothesis that the average slope depends on the long-term difference between uplift and erosion rates. Uplift rates (assumed herefor the purposes of this discussion to be equal to exhumation rates) are lower in the western portion of the SGM and higher in the eastern portion (Spotila et al., 2002, their Fig. 7b). As average slope increases in areas with higher uplift rates, erosion rates increase and soils become thinner. Both of these responses represent negative feedback mechanisms that tend to decrease the differences that would otherwise exist between uplift and erosion rates and between erosion rates and soil production rates. If the uplift rate exceeds the potential soil production rate, soil thickness becomes zero and soil production and erosion rates can no longer increase with increasing slope (in the absence of widespread landsliding in bedrock or intact regolith). In such cases, topography with cliffs or steps may form (e.g., Wahrhaftig, 1965; Strudley et al., 2006; Jessup et al., 2010). However, if the potential soil production rate increases with average slope via the topographically induced stress fracture opening process, the transition to bare landscapes can be delayed or prevented as Heimsath et al. (2012) proposed. This represents an additional negative feedback or adjustment mechanism: beyond the increase in soil production rates in steep terrain made possible by the exponential form of the soil production function. At the highest elevations of the range, soil production is slower, most likely possibly due to temperature limitations on vegetation growth. The interrelationship between these variables can be quantified without explicit knowledge of the uplift rate; since the relationship between soil thickness and average slope implicitly accounts for the uplift rate (i.e., a smaller difference between uplift and erosion rates is characterized by a thinner soil). This conceptual model predicts positive correlations among potential soil

production rates, erosion rates, and topographic steepness, and negative correlations of all of these variables with soil thickness.

Equation (56), in combination with modified versions of equations (9)&(11) of Pelletier and Rasmussen (2009), i.e.,

$$P_r e^{-h/h_0} = E \quad (7)$$

(8)

and

$$\frac{\kappa S_{av}}{1-(S_{av}/S_c)^2} = EL, \quad (89)$$

predict spatial variations in erosion rates and topographic steepness associated with spatial variations in  $P_r$  values. In equations (7)&(8),  $\kappa$  is a sediment transport coefficient ( $\text{m}^2/\text{Myr}$ ) and  $L$  is a mean hillslope length (m). Equation (89) assumes a steady state balance between soil production and erosion, modeled via the nonlinear slope-dependent sediment flux model of Roering et al. (1999) at the hillslope scale. Equation (89) also assumes that the mean slope gradient at the base of hillslopes (where the sediment flux leaves the slope) of a given area can be approximated by the average slope.

Spatial variations in erosion rates can be estimated using  $P_r$  values predicted by equation (56) if spatial variations in soil thickness can also be estimated. To do this, I developed an empirical relationship between soil thickness and slope gradient derived from the Heimsath et al. (2012) dataset (Fig. 6):

$$h = \frac{h_1}{S_{av}^b}, \quad (910)$$

with best-fit coefficients of  $b = 1.0$  and  $h_1 = 0.06$  m ( $R^2 = 0.18$ ,  $p = 0.001$ ). For this regression, I shifted the soil thickness in areas with no soil upward to a small finite value (0.03 m). These areas have no soil today, but must have had some soil over geologic time scale transportable material (i.e., soil) at some point in the past or else no erosion would occur. Also, without some shift, the 10 data points with  $h = 0$

cannot be used, biasing the analysis towards areas that have soil cover today. The 0.03 m value was chosen because this is the minimum finite soil thickness measured by Heimsath et al. (2012).

Using equation (910) as a substitution, equations (7)&(8)&(9) can be combined to obtain a single equation for ~~topographic steepness~~,  $S_{av}$ :

$$\frac{S_{av}}{1-(S_{av}/S_c)^2} = \frac{L}{\kappa} P_{r,pred} \exp\left(-\frac{h_1}{h_0 S_{av}^b}\right) \quad (4011)$$

Given a map of steepness obtained by solving equation (4011), soil thicknesses and erosion rates can be mapped using equations (710) and (8), respectively. Note that the  $S_{av}$  value obtained by solving equation (4011) is not a prediction in the usual sense, since  $S_{av}$  is an input to ~~eqn. (10equation (11))~~ via  $P_{r,pred}$ . ~~The model can be considered to capture the effects of topographic steepness if the predicted and observed values of  $S_{av}$  have broadly similar absolute values and patterns of spatial variation.~~

Equations (7)&(8)&(9) are the same as equations (9)&(11) of Pelletier and Rasmussen (2009) except that their equation (9) included a term representing the bedrock-soil density contrast related to a slightly different definition of  $P_r$  (termed  $P_0$  in Pelletier and Rasmussen (2009)) and their equation (11) assumed a depth- and slope-dependent transport relation. Here I use a ~~slope-dependent soil-depth-independent transport~~ relation because ~~depth-dependentsuch~~ models ~~depend on~~ are highly sensitive to the average soil depth when presence/absence of soil is present (because and areas of thin or no soil must be present for transport to occur), which cannot be determined for locations where are likely to have episodic cover (e.g., rapid mass wasting following incipient soil thickness is currently zero production) that makes measuring or estimating long-term-averaged soil depths difficult.

The  $S_{av}$  values predicted by equation (4011) (Fig. 7C) reproduce the observed first-order patterns of topographic steepness (Fig. 7C) if  $L/\kappa = 0.005$  Myr/m and  $S_c = 0.8$  are used. The value  $S_c = 0.8$  was chosen because it is in the middle of the range of values (i.e., 0.78-0.83) that Grieve et al. (2016) obtained for steep landscapes in California and Oregon. With this value for  $S_c$ , the best-fit value for  $L/\kappa$  was determined by minimizing the least-squares error between the model prediction (Fig. 7B) and observed

variations in average slope (Fig. 7C). Predicted and measured  $S_{av}$  values are lowest in the Western block and higher in the Sierra Madre, Tujunga, and Baldy blocks. Soil thicknesses predicted by the model correlate inversely with slopes and  $P_0P_r$  values (Fig. 7D). Erosion rates (Fig. 7E) closely follow  $P_r$  values, but are lower in absolute value, reflecting the buffering effect of soil on bedrock physical weathering processes.

The model can be further tested by comparison to the catchment-averaged erosion rates reported by DiBiase et al. (2010). Figure 8 plots catchment-averaged erosion rates (unfilled circles) as a function of catchment-averaged  $S_{av}$  values. As with the  $P_r$  values plotted in Figure 2C, I averaged the data in bins of slope in order to minimize local variability related to factors besides average slope. The solid curve represents the model prediction for erosion rate, i.e., equation (8) with  $P_r$  values predicted by equation (5) and  $h$  values predicted by equation (10). Catchment-averaged erosion rates follow a similar pattern as predicted values, remaining constant or increasing slightly with increasing  $S_{av}$  until  $S_{av} \approx 30^\circ$ , beyond which erosion rates increase abruptly. The similarity between  $E$  and  $P_r$  values (Figs. 8 and 2) reflects the important influence of  $S_{av}$  on both variables, the coupling between these variables (i.e., in the absence of widespread landsliding in bedrock or intact regolith, soil must be produced in order for erosion to occur), and the modest impact that differences in soil thickness have on soil production rates across landscapes of different relief in the SGM. Except for several data points of relatively high erosion rates at both the lowest ( $S_{av} = 10-15^\circ$ ) and highest slopes ( $S_{av} > 35^\circ$ ), the model reproduces the absolute values and the slope dependence of the measured erosion rates reasonably well. The underprediction of the model at the highest slopes may be due, in part, to the fact that the  $P_r$  values used to calibrate the model has relatively few data points near the highest end. For example, 4 of 57  $P_r$  values are above 500 m/Myr, while 11 of 50 catchments have erosion rates above this value. The comparison of the predicted curve to the model is not meant to imply that the model prediction is the best or only mathematical expression that represents the data. Rather, Figure 8 (and Figure 2 for the model-data comparison of  $P_r$  values) is intended only to

demonstrate consistency with the threshold increase at  $S_{av} \approx 30^\circ$  predicted by the Savage and Swolfs (1986) model.

### 3 Discussion

This paper adopts a stepwise regression and cluster analysis approach that builds upon the regression analysis that Heimsath et al. (2012) used to characterize the dependence of soil production rate on soil thickness. Stepwise regression is ~~a standard approach in statistics in which the residuals of a statistical regression are computed and additional controls tested for~~ the process of computing the residuals of a regression and testing for additional controls, via additional regression and the calculation of a new set of residuals, until no additional explanatory variable can be identified. Stepwise regression is one method for testing the residuals of a regression for additional controls, which is a recommended step in all regression analyses. I did not apply simultaneous multivariate linear regression (with or without log transformation) because such an approach would have been inconsistent with the complex nonlinear relationships in the data documented by Heimsath et al. (2012) and the analyses presented here.

Estimating  $P_r$  values using the residuals of the regressions of Heimsath et al. (2012) assumes that  $h_0$  has sufficiently limited variation within the two subsets of the study site considered by Heimsath et al. (2012) (i.e., those with  $S_{av}$  values above and below  $30^\circ$ ) that any such variation would not affect the conclusions of the paper. For example, in order for the relationship between  $P_r$  and  $S_{av}$  (i.e., Figs. 2A-2C) to be significantly affected by variations in  $h_0$ ,  $h_0$  would have to have a systematic dependence on  $S_{av}$ . For example, if systematically lower values of  $h_0$  occur at steeper slopes and this effect is not accounted for, the result could be a biasing of  $P_r$  values downward in such regions. Heimsath et al. (2012) clearly demonstrated that no such systematic dependence exists. These authors considered two end member

slope regimes and found that the average  $h_0$  values for these two regions differed by only 0.05 m (0.32 m vs. 0.37 m). At a soil thickness of 0.3 m, this difference corresponds to  $P_r$  differences of approximately 10% (i.e.,  $\exp(-0.30/0.32)$  vs.  $\exp(-0.30/0.37)$ ). This difference is more than 100 times smaller than the variation in  $P_r$  values. The difference becomes even smaller for soils thinner than 0.3 m.

Savage and Swolfs (1986) used a convex-concave geometry, defined by a conformal transformation, in which the slope increases linearly with distance from the divide to the steepest point on the hillslope. In higher-relief portions of the SGM characterized by more planar hillslopes, slopes increase abruptly over a relatively short distance from the ridgetop, then more slowly with increasing distance from the ridgetop. This difference introduces some uncertainty into the application. The model might overestimate the magnitude of topographically induced stress in high-relief portions of the SGM because a more planar slope has a lower curvature than a more parabolic slope and larger curvatures tends to increase extensional stress. On the other hand, more planar hillslopes localize curvature near the ridgetops, which might tend to increase bending stresses that drive extension over and above that predicted by the model for locations near ridgetops.

The effect of topographically induced stresses on ~~regolith~~the production of intact regolith or soil is a rapidly evolving field at the boundaries among geomorphology, geophysics, and structural geology. The results presented here, based on the Savage and Swolfs (1986) model, represents just one possible approach to the problem. Miller and Dunne (1998), for example, modified the Savage and Swolfs (1986) solutions to account for cases with vertical compressive stress gradients (their parameter  $k$ ) larger than 1. Data from the SGM and the adjacent southwestern Mojave Desert indicate that the vertical gradient of horizontal stress in the SGM is likely less than one-, so the modification of Miller and Dunne (1998) may not be necessary for the SGM. Sbar et al. (1979) measured mean maximum compressive stresses at the surface equal to 16 MPa, which is similar to values measured at depths of 100-200 m obtained by Zoback et al. (1980) (their Figs. 7&10). ~~As such, the Savage and Swolfs (1986) approach is likely to be~~

~~appropriate for the SGM.~~ In addition to the effects of variations in the depth gradient of stress, fractures can open beneath hillslopes in a direction perpendicular to the slope, parallel to the slope, or in shear. The criteria for each of these strains depends on different components ~~and/or~~ derivatives of the stress field. For example, Martel (2006, 2011) emphasized the vertical gradient of vertical stress, which depends on the topographic curvature instead of the slope, in driving fracturing parallel to the surface, while St. Clair et al. (2015) emphasized the ratio of the horizontal stress to the spacing between ridges and valleys. More research is needed in the SGM and elsewhere to better understand the response of bedrock and intact regolith to the 3D stress field. However, all studies agree that the extent of one or more fracture opening modes increases with topographic slope and/or curvature, often with a threshold change from compression to tension above a critical value of topographic ruggedness.

The results presented here provide a possible process-based understanding of the dependence of potential soil production rates on topographic steepness documented by Heimsath et al. (2012) in the SGM. These authors proposed a negative feedback in which high erosion rates trigger higher potential soil production rates, with the result that soil cover may more persistent than previously thought. The results presented here show that previous models of topographically induced stresses suggest that transitions from compressive to tensile strength at hillslope angles similar to those at which  $P_c$  values increase. This similarity suggests that in the SGM, the release of compressive stress in steep landscapes causes/may cause fractures beneath ridges to open, thereby allowing weathering agents to penetrate into the bedrock or intact regolith more readily. The fact that this process requires a regional compressive stress state suggests that ~~this~~ it is not likely to be equally important everywhere on Earth. In cases of low regional compression or extension, the development of rugged topography in rocks with pre-existing fractures is not likely to be significant in promoting fracture opening in the rocks beneath hillslopes.

Heimsath et al. (2012) argued that  $P_r$  values (analogous to what they termed  $SPR_{max}$  values) increase with erosion rates not just in the SGM, but globally based on the strong correlation between  $P$  and  $E$  values (their Fig. 4b). However, the results of this paper ~~suggest that it is slope that controls  $P_r$  values, not erosion rate. Slope and erosion rate are highly correlated in the SGM, but this correlation is not universal. The results of this paper also suggest that the process by which slope leads to an argue against a global~~ increase in  $P_r$  values with  $E$  values ~~in the SGM~~. The process described in this paper, i.e., ~~topographically induced compressive stress opening of fractures~~ is likely not operative ~~in reduction near ridgetops in compressive-stress environments, does not apply to~~ extensional or neutral-stress settings. As such, other factors might explain the global correlation between  $P$  and  $E$  values. For example, erosion rates may be limited by  $P_r$  values (since erosion cannot occur faster than soil is produced in the absence of widespread landsliding in bedrock or intact regolith). Also,  $P_r$  values are a function of climate, with values exceeding 1000 m/Myr in humid climates (Pelletier and Rasmussen, 2009; Larsen et al., 2014). As such, the global correlation between  $P$  and  $E$  values may, in part, be a result of water availability being important for both soil production and erosion processes. If ~~erosion~~ soil production rates cannot keep pace with erosion rates, stepped topography can and does form in ~~some~~ many cases (e.g., Wahrhaftig, 1965; Strudley et al., 2006; Jessup et al., 2010), leading to a reduction in erosion rates (as evidenced by lower soil production rates in bare areas relative to soil-covered areas (Hahm et al., 2014)) despite locally steeper slopes. In such cases,  $P$  and  $E$  values are still correlated because erosion cannot occur at rates higher than  $P_r$ .

#### 4 Conclusions

In this paper I estimated spatial variations in the potential soil production rate,  $P_r$ , using cosmogenic-radionuclide-derived soil production rates from the central San Gabriel Mountains of

California published by Heimsath et al. (2012). The results demonstrate that trends in the data are consistent with the hypothesis that topographically induced stresses cause pre-existing fractures to open beneath steeper hillslopes. This model predicts an abrupt increase in  $P_r$  values close to the average slope (approximately  $30^\circ$ ) where an increase is observed in the data. After the effects of topographically induced stress are accounted for, a limitation on  $P_r$  values ~~can be detected~~ is detectable at the highest elevations of the range, where vegetation growth is limited by temperature. There is some evidence that lithology and local fault density may also influence potential soil production rates, but the null hypotheses that these processes are not significant cannot be ruled out with given a threshold statistical significance (false positive rate) of 0.05, or they cannot be clearly distinguished from other controls. The results of this paper demonstrate that  $P_r$  values ~~are~~ may be solely dependent on climate and rock characteristics as has been traditionally assumed, but that rock characteristics evolve with topographic ruggedness in compressive-stress environments. These results provide a useful foundation for additional targeted cosmogenic-radionuclide analyses in the San Gabriel Mountains and for the incorporation of methods that can further test the topographically induced stress fracture opening hypothesis such as shallow seismic refraction surveys and 3D stress modeling.

## Acknowledgements

I thank Katherine Guns for drafting Fig. 1. I wish to thank Arjun Heimsath, Kelin Whipple, Simon Mudd, Jean Braun, and ~~four~~ six anonymous reviewers for ~~critical~~ reviews of this and earlier versions of the manuscript.

## References

Chester, J.S., Chester, F.M., and Kronenberg, A.K.: Fracture surface energy of the Punchbowl fault, San Andreas system, *Nature*, 437, 133–136, doi:10.1038/nature03942, 2005.

Daly, C., Taylor, G.H., Gibson, W.P., Parzybok, T.W., Johnson, G.L., and Pasteris, P.: High-quality spatial climate data sets for the United States and beyond, *Trans. Am. Soc. Ag. Eng.*, 43: 1957–1962, doi:10.13031/2013.3101, 2001.

DiBiase, R.A., Heimsath, A.M., and Whipple, K.X.: Hillslope response to tectonic forcing in threshold landscapes, *Earth Surf. Process. Landf.*, 37, 855–865, doi:10.1002/esp.3205, 2012.

DiBiase, R.A. and Whipple, K.X.: The influence of erosion thresholds and runoff variability on the relationships among topography, climate, and erosion rate, *J. Geophys. Res. Earth Surf.*, 116, F04036, doi:10.1029/2011JF002095, 2011.

DiBiase, R.A., Whipple, K.X., and Heimsath, A.M.: Landscape form and millennial erosion rates in the San Gabriel Mountains, CA, *Earth Planet. Sci. Lett.*, 289(1-2), 134–144, doi:10.1016/j.epsl.2009.10.036, 2010.

DiBiase, R.A., Whipple, K.X., Lamb, M.P., and Heimsath, A.M.: The role of waterfalls and knickzones in controlling the style and pace of landscape adjustment in the western San Gabriel Mountains, California, *Geol. Soc. Am. Bull.*, 127(3-4), 539–559, doi:10.1130/B31113.1, 2015.

Dixon, J.L., Hartshorn, A.S., Heimsath, A.M., DiBiase, R.A., and Whipple, K.X.: Chemical weathering response to tectonic forcing: A soils perspective from the San Gabriel Mountains, California, *Earth Planet. Sci. Lett.*, 323, 40–49, doi:10.1016/j.epsl.2012.01.010, 2012.

Goodfellow, B.W., Skelton, A., Martel, S.J., Stroeven, A.P., Jansson, K.N., and Hättestrand, C.: Controls of tor formation, Cairngorm Mountains, Scotland, *J. Geophys. Res. Earth Surf.*, 119, 225–246, doi:10.1002/2013JF002862, 2014.

Grieve, S.W.D., Mudd, S.M., Hurst, M.D., and Milodowski, D.T.: A nondimensional framework for exploring the relief structure of landscapes, *Earth Surf. Dynam.*, 4, 309–325, doi:10.5194/esurf-4-309-2016, 2016.

Griffiths, P.G., Webb, R.H., and Melis, T.S.: Frequency and initiation of debris flows in Grand Canyon, Arizona, *J. Geophys. Res.*, 109, F04002, doi:10.1029/2003JF000077, 2004.

Hahm W.J., Riebe, C.S., Lukens, C.E., Araki, S.: Bedrock composition regulates mountain ecosystems and landscape evolution, *Proc. Nat. Acad. Sci. USA*, 111, 3207–3212. doi:10.1073/pnas.1315667111, 2014.

Heimsath, A.M., DiBiase, R.A., and Whipple, K.X.: Soil production limits and the transition to bedrock dominated landscapes, *Nature Geosci.*, 5, 210–214, doi:10.1038/ngeo1380, 2012.

Jessup, B.S., Miller, S.N., Kirchner, J.W., and Riebe, C.S.: Erosion, Weathering and Stepped Topography in the Sierra Nevada, California; Quantifying the Dynamics of Hybrid (Soil-Bedrock) Landscapes, American Geophysical Union, Fall Meeting 2010, abstract #EP41D-0736, 2010.

Koons, P.O., Upton, P., and Barker, A.D.: The influence of mechanical properties on the link between tectonic and topographic evolution, *Geomorphology*, 137(1), 168–180, doi:10.1016/j.geomorph.2010.11.012, 2012.

Larsen, I.J., Almond, P.C., Eger, A., Stone, J.O., Montgomery, D.R., and Malcolm, B.: Rapid soil production and weathering in the Southern Alps, New Zealand, *Science*, 343(6171), 637–640, doi:10.1126/science.1244908, 2014.

Lifton N.A., and Chase, C.G.: Tectonic, climatic and lithologic influences on landscape fractal dimension and hypsometry: implications for landscape evolution in the San Gabriel Mountains, California, *Geomorphology*, 5(1-2), 77–114, doi:10.1016/0169-555X(92)90059-W, 1992.

- Martel, S.J.: Effect of topographic curvature on near-surface stresses and application to sheeting joints, *Geophys. Res. Lett.*, 33, L01308, doi:10.1029/2005GL024710, 2006.
- Martel, S.J.: Mechanics of curved surfaces, with application to surface-parallel cracks, *Geophys. Res. Lett.*, 38, L20303, doi:10.1029/2011GL049354, 2011.
- Miller, D.J., and Dunne, T.: Topographic perturbations of regional stresses and consequent bedrock fracturing, *J. Geophys. Res.*, 101(B11), 25523–25536, doi:10.1029/96JB02531, 1996.
- Molnar, P.: Interactions among topographically induced elastic stress, static fatigue, and valley incision, *J. Geophys. Res.*, 109, F02010, doi:10.1029/2003JF000097, 2004.
- Molnar, P., Anderson, R.S., and Anderson, S.P.: Tectonics, fracturing of rock, and erosion, *J. Geophys. Res. Earth Surf.*, v. 112, F03014, doi:10.1029/2005JF000433, 2007.
- Morton, D.M., and Miller, F.K.: Preliminary Geologic Map of the San Bernardino 30'x60' Quadrangle, California, v. 1.0, U.S. Geological Survey Open-File Report 03-293, Reston, Virginia, 2003.
- Nourse, J.A.: Middle Miocene reconstruction of the central and eastern San Gabriel Mountains, southern California, with implications for evolution of the San Gabriel fault and Los Angeles basin, in Barth, A., ed., *Contributions to the Crustal Evolution of the Southwestern United States*: Boulder, Colorado, Geological Society of America Special Paper 365, 161–185, 2002.
- Pelletier, J.D., and Rasmussen, C.: Quantifying the climatic and tectonic controls on hillslope steepness and erosion rate, *Lithosphere*, 1(2), 73–80, doi:10.1130/L3.1, 2009.
- Roering, J.J., Kirchner, J.W., and Dietrich, W.E.: Evidence for nonlinear, diffusive sediment transport on hillslopes and implications for landscape morphology, *Water Resour. Res.*, 35(3), 853–870, doi:10.1029/1998WR900090, 1999.
- Roering, J.J., Kirchner, J.W., and Dietrich, W.E.: Characterizing structural and lithologic controls on deep-seated landsliding: Implications for topographic relief and landscape evolution in the

- Oregon Coast Range, USA, *Geol. Soc. Am. Bull.*, 117(5/6), 654–668, doi:10.1130/B25567.1, 2005.
- Roy, S.G., Koons, P.O., Upton, P., and Tucker, G.E.: Dynamic links among rock damage, erosion, and strain during orogenesis, *Geology*, 44(7), 583–586, doi:10.1130/G37753.1, 2016a.
- Roy, S.G., Tucker, G.E., Koons, P.O., Smith, S.M., and Upton, P.: A fault runs through it: Modeling the influence of rock strength and grain-size distribution in a fault-damaged landscape, *J. Geophys. Res. Earth Surf.*, 121, 1911–1930, doi:10.1002/2015JF003662, 2016b.
- Savage, H.M., and Brodsky, E.E.: Collateral damage: Evolution with displacement of fracture distribution and secondary fault strands in fault damage zones, *J. Geophys. Res.*, 116, B03405, doi:10.1029/2010JB007665, 2011.
- Savage, W.Z., Swolfs, H.S., and Powers, P.S.: Gravitational stresses in long symmetric ridges and valleys: *Int. J. Rock Mech. Min. Sci. & Geomech. Abs.*, 22(5), 291–302, 1985.
- Savage, W.Z., and Swolfs, H.S.: Tectonic and gravitational stress in long symmetric ridges and valleys: *J. Geophys. Res.*, v. 91, p. 3677–3685, 1986.
- Sbar, M.L., Richardson, R.M., Flaccus, C., and Engelder, T.: Near-surface in situ stress: 1. Strain relaxation measurements along the San Andreas Fault in southern California, *J. Geophys. Res.*, 89(B11), 9323–9332, doi:10.1029/JB089iB11p09323, 1984.
- Spotila, J.A., House, M.A., Blythe, A.E., Niemi, N.A., and Bank, G.C.: Controls on the erosion and geomorphic evolution of the San Bernardino and San Gabriel Mountains, southern California, in Barth, A., ed., *Contributions to Crustal Evolution of the Southwestern United States*: Boulder, Colorado, Geological Society of America Special Paper 365, 205–230, 2002.
- Strudley, M.W., Murray, A.B., and Haff, P.K.: Regolith thickness instability and the formation of tors in arid environments, *J. Geophys. Res.*, 111, F03010, doi:10.1029/2005JF000405, 2006.

U.S. Geological Survey: LANDFIRE database, digital data available at <http://www.landfire.gov/>, accessed July 5, 2016.

U.S. Geological Survey and California Geological Survey: Quaternary fault and fold database for the United States, digital data available at <http://earthquakes.usgs.gov/regional/qfaults/>, accessed July 5, 2016.

Wahrhaftig, C.: Stepped topography of the southern Sierra Nevada, California, *Geol. Soc. Am. Bull.*, 76(10), 1165–1190, doi: 10.1130/0016-7606(1965)76[1165:STOTSS]2.0.CO;2, 1965.

Yang, W. and Hauksson, E.: The tectonic crustal stress field and style of faulting along the Pacific North America Plate boundary in Southern California, *Geophys. J. Int.*, doi:10.1093/gji/ggt113, 2013.

Yerkes, R.F. and Campbell, R.H.: Preliminary Geologic Map of the Los Angeles 30' x60' Quadrangle, Southern California, v. 1.0, U.S. Geological Society Open-File Report 2005-1019, Reston, Virginia, 2005.

Zoback, M.D., Tsukahara, H., and Hickman, S., Stress measurements at depth in the vicinity of the San Andreas Fault: Implications for the magnitude of shear stress at depth, *J. Geophys. Res.*, 85(B11), 6157–6173, doi:10.1029/JB085iB11p06157, 1980.

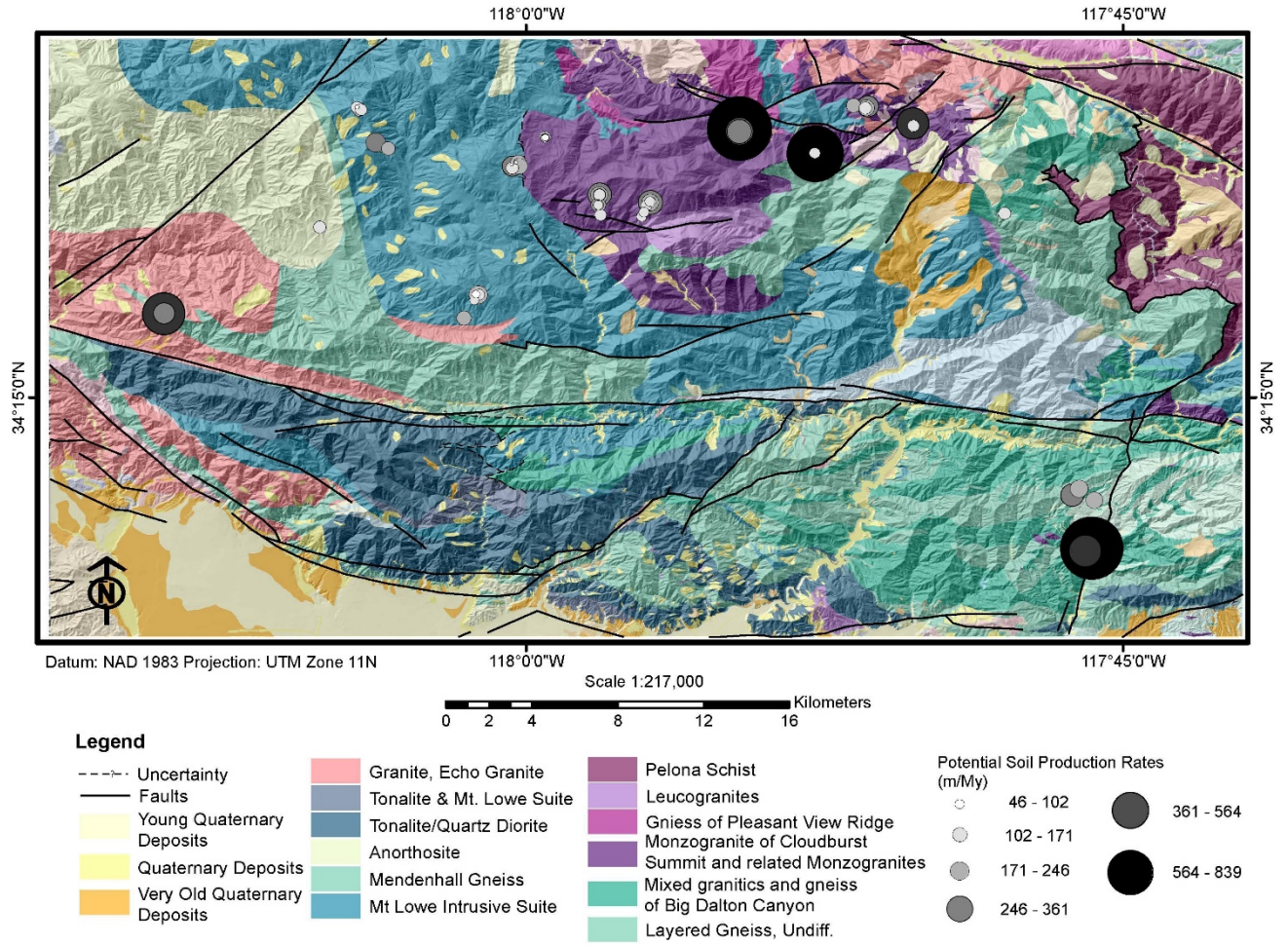


**Figure 1. Geologic map of the central San Gabriel Mountains, California. Potential soil production rates inferred from the data of Heimsath et al. (2012) are also shown. Lithologic units were compiled using Yerkes and Campbell (2005), Morton and Miller (2003), and Figure 3 of Nourse (2002). Faults were mapped from Morton and Miller (2003) and the Quaternary fault and fold database of the United States (U.S. Geological Survey and California Geological Survey, 2006).**

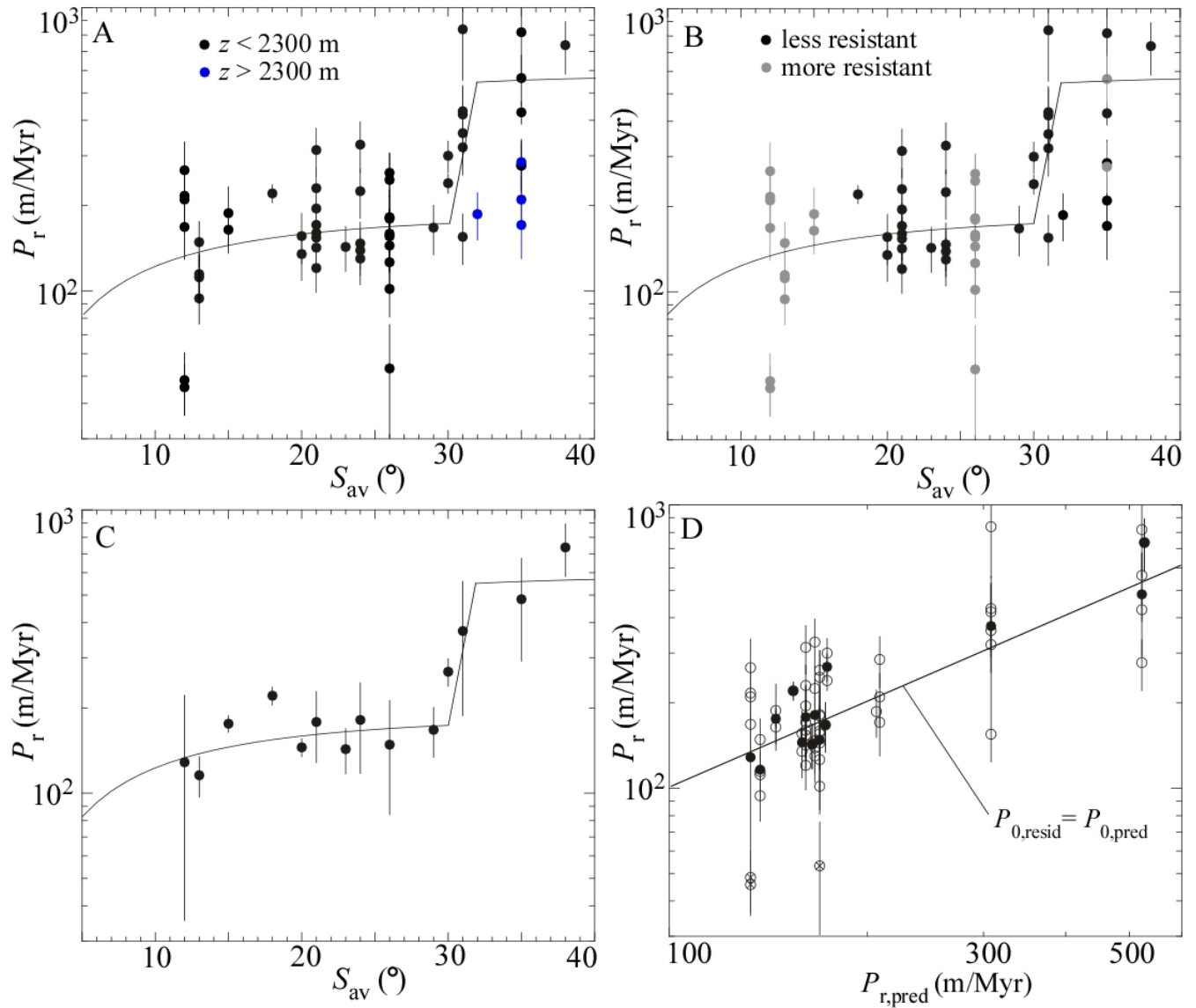
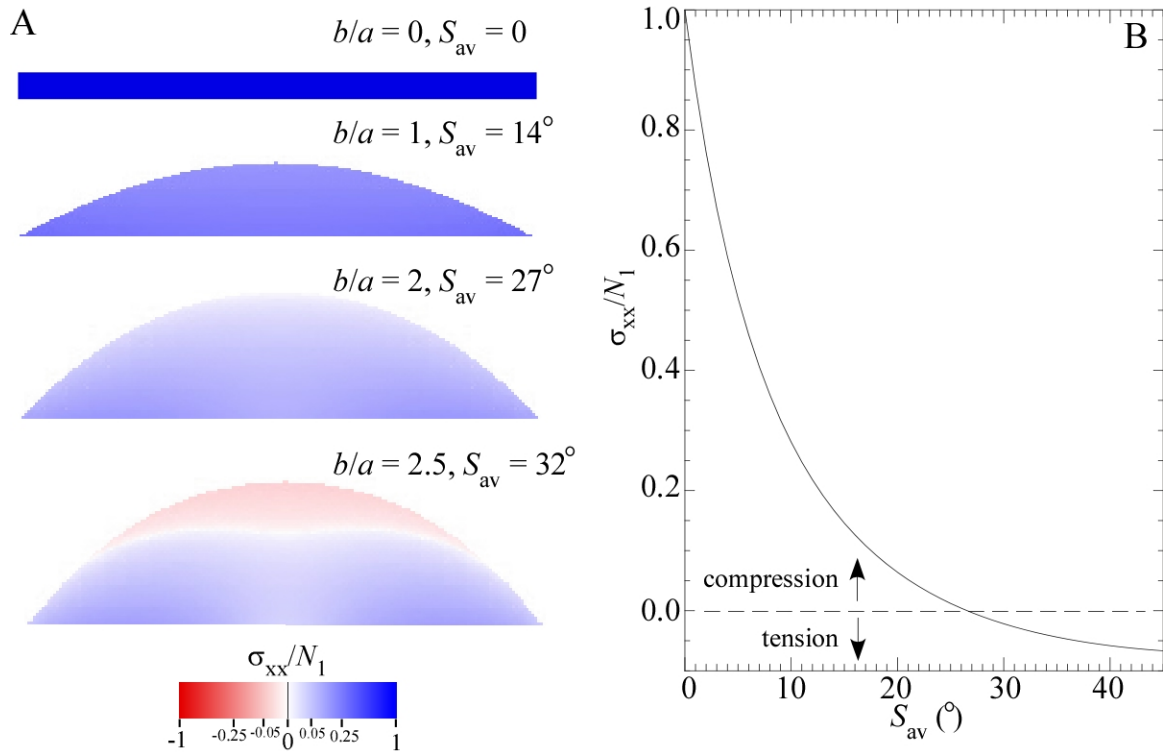
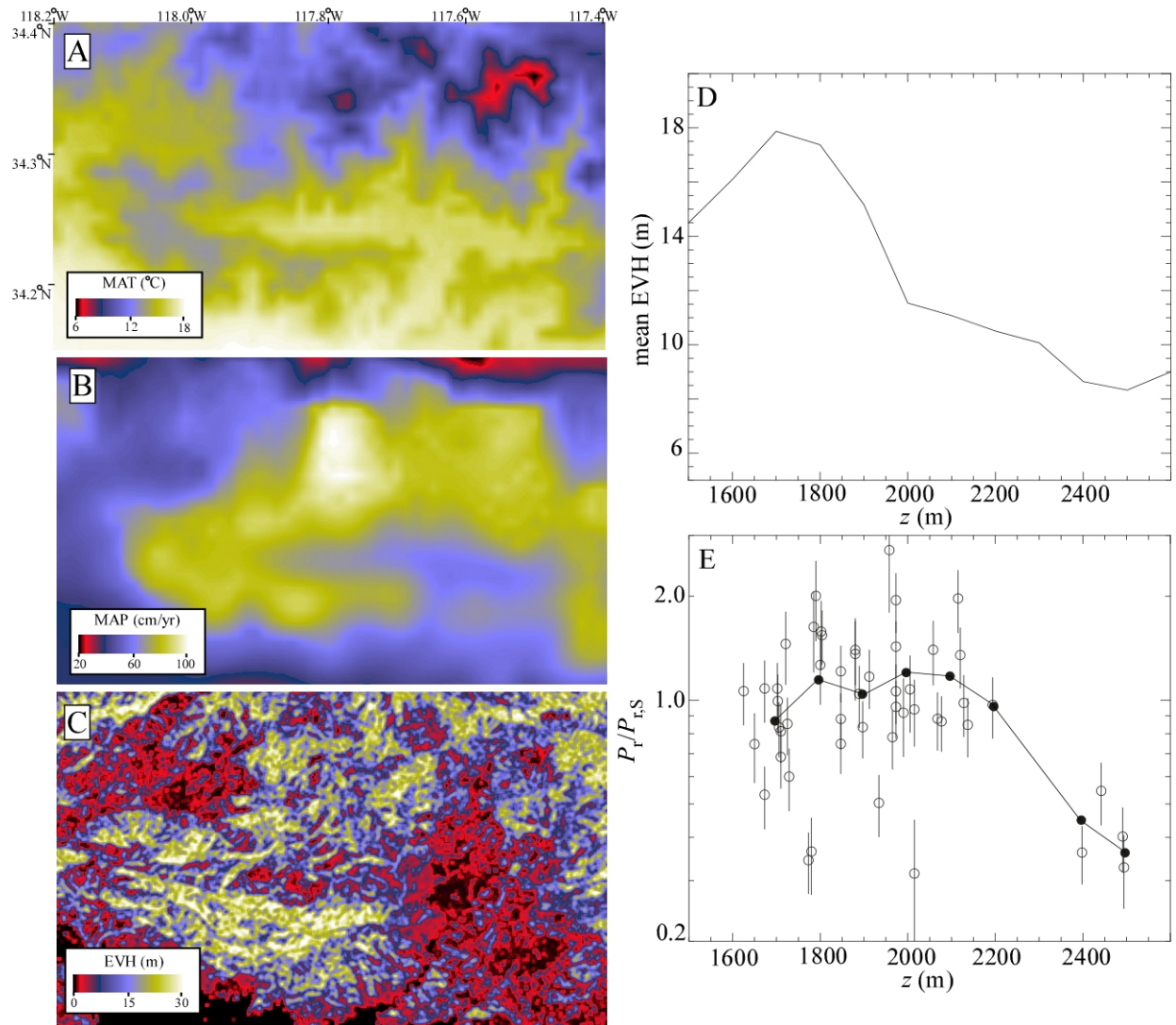


Figure 2. Plots of  $P_r$  and their relationship to average slope,  $S_{av}$ , and other potential controlling factors. (A) Plot of  $P_r$  values versus  $S_{av}$ . Data points colored blue are from the highest elevations of the range ( $z > 2300$  m). **The piece-wise curve plots equation (4), with the three segments of the curve corresponding to the three conditions in the equation.** (B) The same plot as (A), except that data points are colored according to whether they from rocks that are relatively more resistant (gray) or less resistant (black) to weathering. (C) Plot of  $P_r$  values averaged for each value of  $S_{av}$ . In (A) and (B), error bars represent the uncertainty of each data point, while in (C) the error bar represents the standard deviation of the data points averaged for each  $S_{av}$  value. (D) Plot of  $P_r$  versus values predicted from equation (5). Unfilled circles show individual data points, while filled circles represent the averaged data plotted in (C).



**Figure 3. Analytic solutions illustrating the perturbation of a regional compressive stress field by topography. (A) Color maps of the horizontal normal stress,  $\sigma_{xx}$  (normalized to the regional stress,  $N_1$ ), as a function of ridge steepness (defined by the shape factor  $b/a$  of Savage and Swolfs (1986) and the average slope  $S_{av}$ ) using equations (34) and (35) of Savage and Swolfs (1986). The hillslopes are plotted with no vertical exaggeration. (B) Plot of  $\sigma_{xx}$  directly beneath the ridge as a function of  $S_{av}$  using equation (36) of Savage and Swolfs (1986). The plot illustrates the decrease in compressive stress with increasing average slope and the transition to tensile stresses at a  $S_{av}$  value of approximately  $27^\circ$ .**



**Figure 4. Climate and vegetation cover of the central San Gabriel Mountains. Color maps of (A) mean annual temperature (MAT) and (B) mean annual precipitation (MAP) from the PRISM dataset (Daly et al., 2001). (C) Color map of mean existing vegetation height (EVH) from the U.S. Geological Survey LANDFIRE database (U.S.G.S., 2016). (D) Plot of mean EVH versus elevation above sea level,  $z$ , using the data illustrated in (C). (E) Plot of the ratio of  $P_r$  to  $P_{r,s}$  as a function of elevation. Filled circles are binned averages of the data (each bin equals 100 m in elevation).**

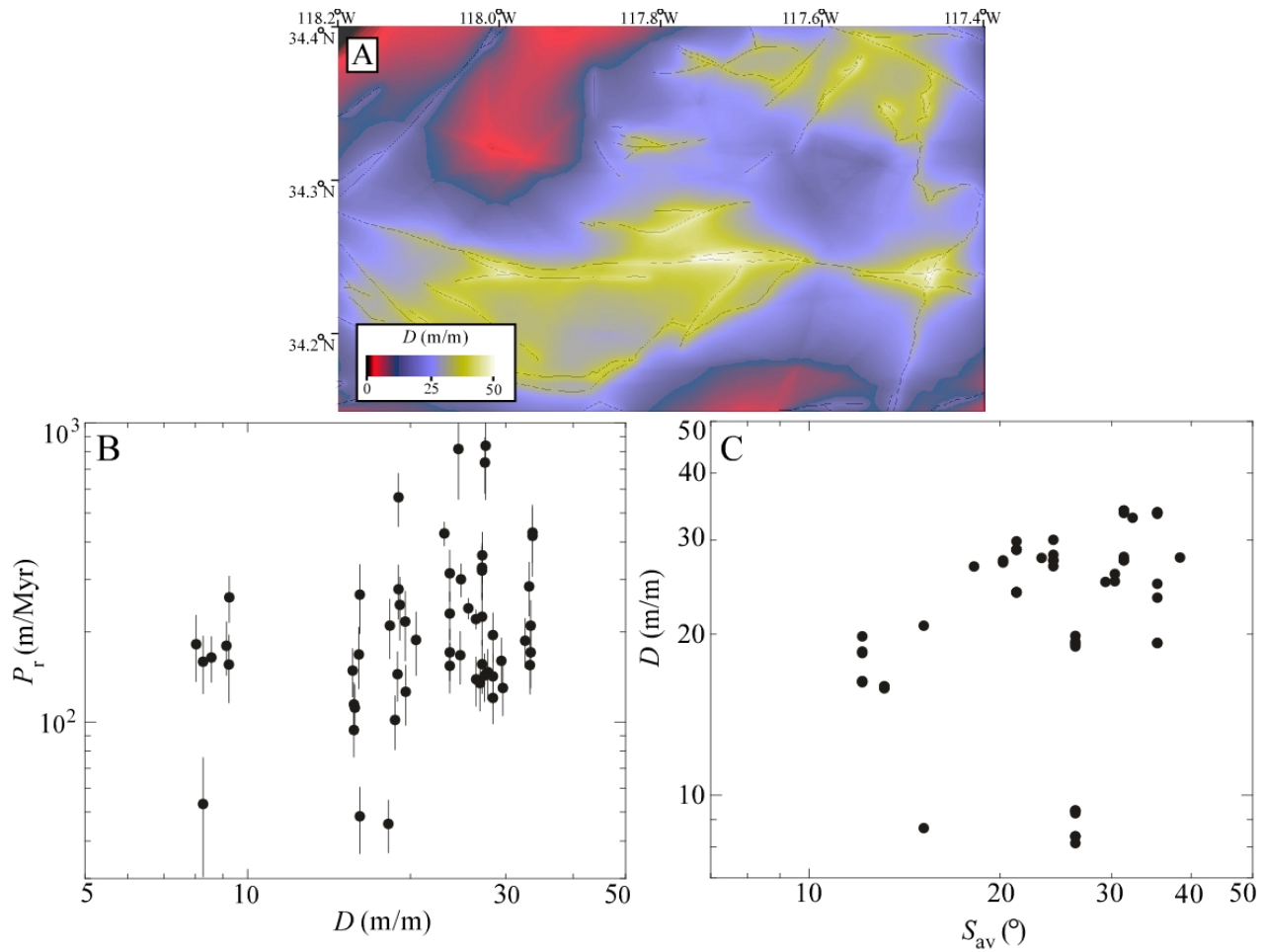
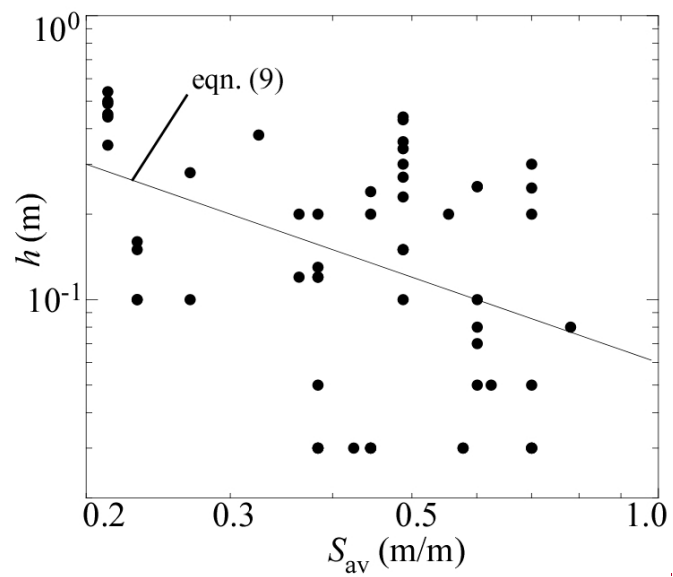


Figure 5. Map of the bedrock damage index,  $D$ , and its correlation with  $S_{av}$ . (A) Color map of spatial variations  $D$ . (B) Plot of  $D$  versus  $S_{av}$  for the 57 sample locations of Heimsath et al. (2012).



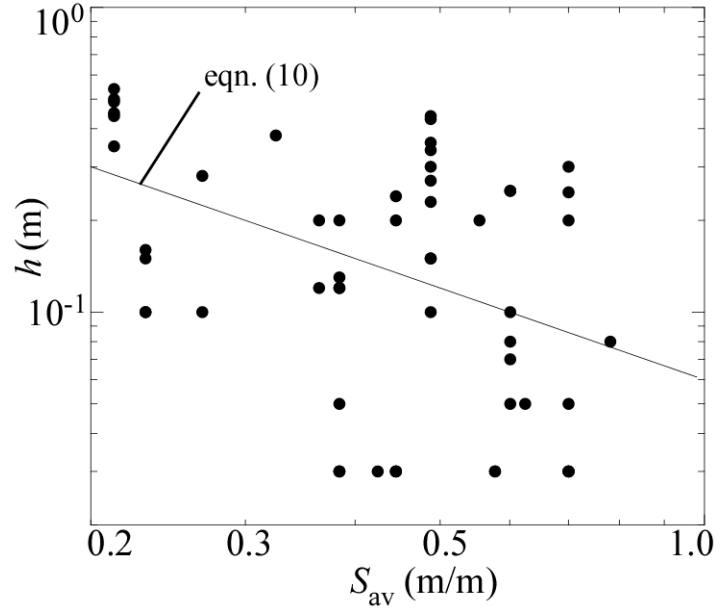


Figure 6. Plot of soil thickness,  $h$ , as a function of average slope,  $S_{av}$ . The least-squares power-law fit to the data (~~equation~~ ~~(9eqn. (10))~~) is also shown.

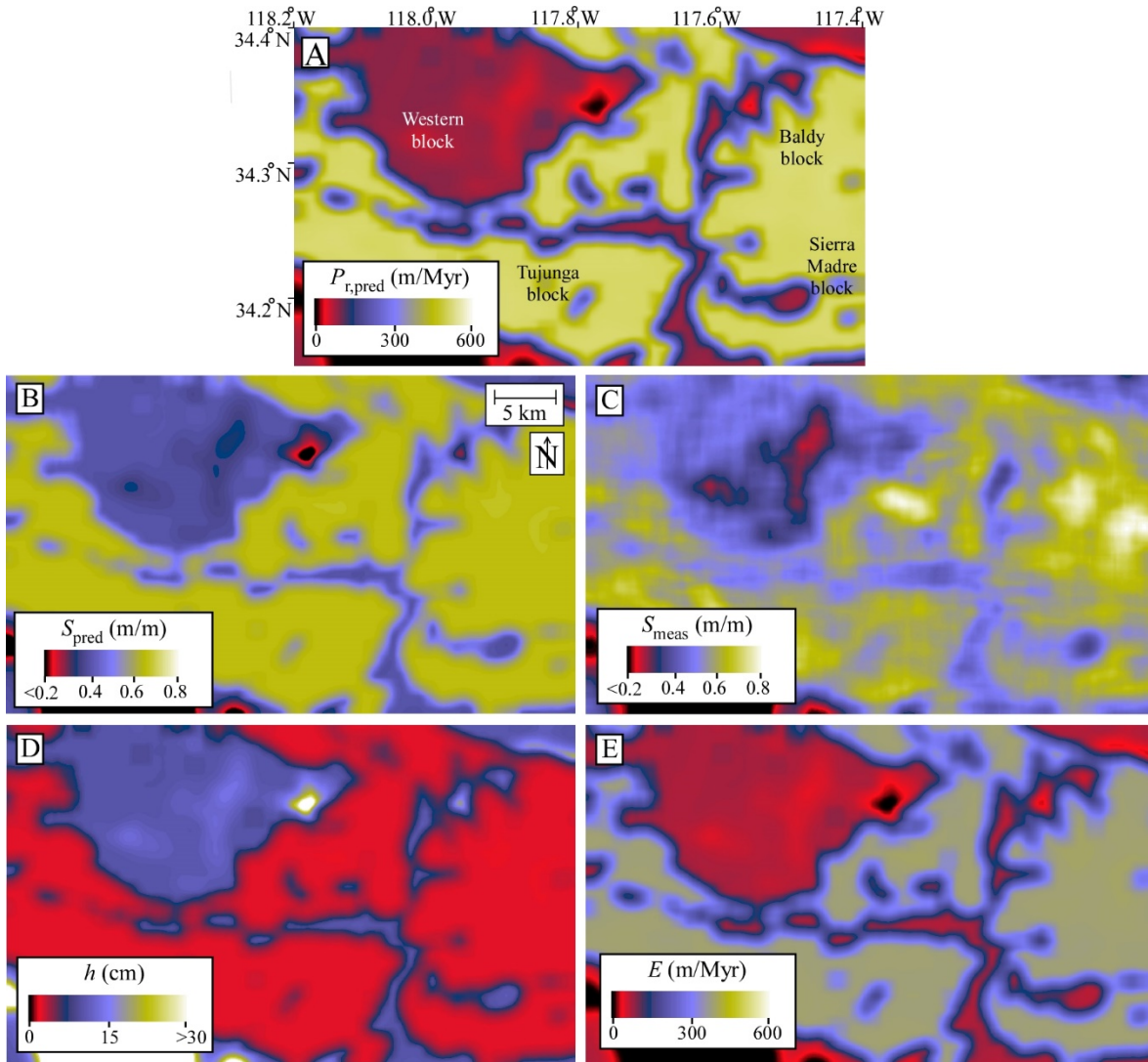
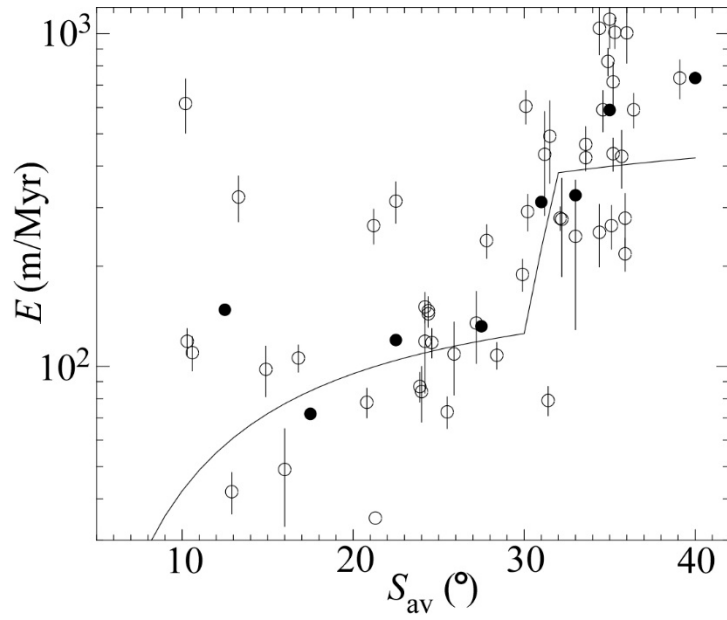


Figure 7. Color maps illustrating the predicted potential soil production rate from equation (56) ( $P_{r,pred}$ ), predicted and observed values of average slope,  $S_{av}$ , soil thickness,  $h$ , and erosion rate,  $E$ . (A) Color map of  $P_{r,pred}$  values estimated from equation (56). (B) Color map of  $S_{av}$  values predicted by equation (1011), smoothed by a moving average filter with a 1-km length scale to emphasize patterns at the landscape scale. (C) Color map of actual (DEM-derived)  $S_{av}$  values, smoothed in the same manner as (B). (D) Color map of soil thicknesses,  $h$ , predicted by equation (910). (E) Color map of erosion rates,  $E$  predicted by equation (78).



**Figure 8.** Plot of the catchment-averaged erosion rates of DiBiase et al. (2010) (unfilled circles) versus catchment-averaged  $S_{av}$ . Filled circles represent log-transformed averages of data within the following bins: 10-15°, 15-20°, 20-25°, 25-30°, 30-32°, 32-34°, and 34-36°. The curve plots the model prediction, i.e., equation (8) with  $P_r$  values predicted by eqn. (5) and  $h$  values predicted by equation (10).